Title
FACTORS CONTROLLING WETTING OF MAGNESIUM OXIDE BY SILICATE LIQUIDS

Author
Aksay, Ilhan Arif.

Publication Date
1969-03-01

UCRL-18766

eg 2

FACTORS CONTROLLING WETTING OF MAGNESIUM OXIDE BY SILICATE LIQUIDS

Ilhan Arif Aksay
(M.S. Thesis)

March 1969

AEC Contract No. W-7405-eng-48

LAWRENCE RADIATION LABORATORY
UNIVERSITY of CALIFORNIA BERKELEY

eg 2

UCRL-18766

DISCLAIMER

FACTORS CONTROLLING WETTING OF MAGNESIUM OXIDE
BY SILICATE LIQUIDS

Contents

FACTORS CONTROLLING WETTING OF MAGNESIUM OXIDE BY SILICATE LIQUIDS

Ilhan Arif Aksay

Inorganic Materials Research Division, Lawrence Radiation Laboratory, and Department of Materials Science and Engineering, College of Engineering, University of California, Berkeley, California

ABSTRACT

March 1969

The effect of Al_2O_3, Cr_2O_3, Fe_2O_3, and TiO_2 additions on the solid-liquid interfacial energy of the magnesium oxide-monticellite ($CaO \cdot MgO \cdot SiO_2$) system has been studied. The thermodynamic equilibrium of the magnesium oxide-monticellite system is disturbed with R_2O_3 and TiO_2 additions to the liquid. At the liquid-solid interface, reactions occur in order to achieve an equilibrium composition. The degree of wetting is directly proportional to the magnitude of (-) ΔG of this interface reaction. Therefore, the reported contact angles are the steady state angles of a transient reaction stage.

The contact angle of the monticellite liquid on the (100) face of MgO single crystal was in the range of 43-51° at 1550°C. With additions of Al_2O_3 and Fe_2O_3, the angle decreased to a value of 35° and 15°, respectively. Spreading was obtained with Cr_2O_3 and TiO_2 additions.

I. INTRODUCTION

The need for improved refractories is felt in various industries where operating temperatures are constantly increasing. At the present, especially in the steel making industry, the choice of refractories is very limited. The refractory lining of a furnace has to be resistant to chemical attacks by slags. It also has to be rigid enough to hold the furnace structure together without slumping. Magnesite and chrome-magnesite refractories have been known, through experience, to meet these requirements. During the last decade, an extensive research has been directed to this area in order to understand and consequently to improve the properties of an already promising system.

The high temperature strength of a material in the presence of a liquid phase is determined by the distribution of this liquid phase between the solid particles.[1,2] This liquid can either wet the solid particles and form a film around them or stay in isolated pockets when the liquid does not wet the solid. In a compact the distribution of the liquid is indicated by the "dihedral angles,"[3] shown schematically in Fig. 1(b). At equilibrium, the balance between the solid-liquid interfacial tensions and the grain boundary tension is determined by

$$ {}_s\gamma_s = 2\ {}_s\gamma_\ell \cos(\phi/2) \qquad (1) $$

where ${}_s\gamma_s$ = solid-solid interfacial or grain boundary energy,

${}_s\gamma_\ell$ = solid-liquid interfacial energy, and

ϕ = dihedral angle between solid-liquid, measured through the liquid.

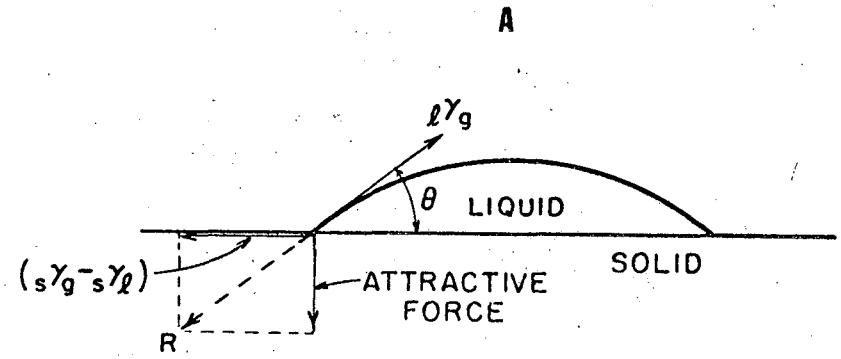

Fig. 1a. Equilibrium of forces acting on the periphery of an acute contact angle.

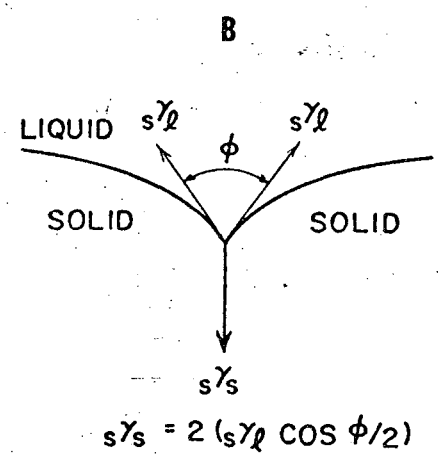

Fig. 1b. Equilibrium between a grain boundary and two equivalent solid-liquid interphase boundaries.

XBL 688-5670

Contact angle measurements with sessile drop experiments also provide useful information on the solid-liquid interfacial energy relative to the solid and liquid surface energies. Under equilibrium conditions, the contact angle, shown in Fig. 1(a), is determined by Young's equation

$$({}_s\gamma_g - {}_s\gamma_\ell) = {}_\ell\gamma_g \cos\theta \qquad (2)$$

where ${}_s\gamma_g$ = solid-gas surface energy, and

θ = contact angle, measured through the liquid phase.

An acute contact angle indicates that the driving force for forming an interface is the lowering of the solid surface energy by the liquid. This force, equal to $({}_s\gamma_g - {}_s\gamma_\ell)$, manifests itself as a horizontal force acting on the periphery of the drop. A low contact angle is usually a good indication that the liquid will wet the solid grains in a compact. The final equilibrium distribution of the phases, however, is still determined by the dihedral angle.

The chrome ore used in the production of chrome-magnesite refractories is primarily a solid solution of $MgFe_2O_4$, $MgCr_2O_4$ and $MgAl_2O_4$ spinels. Chrome grains along with periclase grains constitute the solid phases of these refractories in the presence of a calcium, magnesium silicate liquid. The composition of this liquid is best represented by its CaO/SiO_2 ratio. In a periclase-monticellite ($CaO \cdot MgO \cdot SiO_2$) model system, the effect of Cr_2O_3, Fe_2O_3, Al_2O_3, and TiO_2 additives on the dihedral angle between the periclase grains has recently been determined.[4,5] The results obtained from this model system have been quite helpful in understanding the role of spinels introduced into a chrome-magnesite system with chrome ore.

The goal of this study is to determine the effect of Cr_2O_3, Fe_2O_3, Al_2O_3, and TiO_2 on the solid-liquid interfacial energy of the same periclase-monticellite system. It is hoped that the results of this study will also bring about a greater understanding of the role of interfaces in the development of microstructure.

II. LITERATURE SURVEY

A. Surface and Interface Phenomena

The techniques of measuring surface and interfacial energies at elevated temperatures and the difficulties connected with these techniques have been discussed by Kingery and Humenik,[6] and Kozakévitch.[7] Sessile drop experiments were generally preferred.

Halden and Kingery[8] have studied the liquid iron-Al_2O_3 system with sessile drop experiments in vacuum at 1570°C. The S, O, N, and C additives to the liquid iron were found to adsorb at the surface, and the surface activity decreased in the order: S> O> N> C. Carbon seemed to react with Al_2O_3 at the interface which resulted in a drop in the interfacial energy. The liquid nickel-Al_2O_3 system has been studied by Kurkjian and Kingery[9] with sessile drop experiments at 1475°C. Sn, In, Cr, and Ti were used as additives. Among these additives, only tin and indium changed the surface tension due to adsorption at the surface. Titanium and chromium concentrated at the interface and lowered the interfacial energy. Allen and Kingery[10] have determined surface and interfacial energies in various metal-ceramic systems. The metals used were Fe, Cu, Ni, Co, Sn, Fe-C, Co-C, and Ni-C, and the substrates were Al_2O_3, Si_3N_4, $MoSi_2$, and SiC.

The understanding of chemical reactions at the interface has been emphasized by Kingery[11] as a major task for the fabrication of cermet bodies. Economos and Kingery[12] have investigated the interfacial reactions in metal oxide systems at elevated temperatures and classified them under four groups: (a) formation of a new phase at the interface, (b) corrosion of the oxide by the metal, (c) penetration along the grain

boundaries and diffusion into the bulk, and (d) no physical alteration at the interface. Humenik and Kingery[13] have determined surface tensions and work of adhesion in metal-ceramic systems with sessile drop experiments. They found that the wetting tendency and work of adhesion were increased whenever interfacial reactions occurred. The increase in the wetting tendency and work of adhesion was attributed to a decrease in the interfacial energy caused by a change in the composition of the metal at the interface. The wettability and work of adhesion were also found to increase with low surface tension of the metal and high metal-oxide bond strength. Furthermore, Kingery[14] has determined the interfacial and surface energies of the Ni-Al_2O_3, Ni-ZrO_2, and Fe-Al_2O_3 systems. In the Fe-Al_2O_3 system, with small additions of Si to Fe, chemisorption of Si at the interface was explained on the basis of a greater stability of Si-O bonds as compared to Fe-O bonds.

Armstrong, et al.[15] have performed sessile drop experiments with (Ni-Ti) and (Ni-Cr) alloys on Al_2O_3 at 1500°C. In the (Ni-Ti)-Al_2O_3 system, the interfacial energy decreased approximately 600 ergs/cm^2 when the Ti content of the alloy was increased from 0.2 to 2.0%. In the (Ni-Cr)-Al_2O_3 system, this drop in the interfacial energy was about 750 ergs/cm^2 when the Cr content was increased from 1 to 10%. In each case the drop in the interfacial energy was due to the selective adsorption of Ti and Cr atoms at the interface where in the (Ni-Ti)-Al_2O_3 system the formation of α-Ti_2O_3, and in the (Ni-Cr)-Al_2O_3 system only the diffusion of Cr into Al_2O_3 were observed. Armstrong, et al.[16,17] have also studied interface reactions in SiO_2-refractory metal (Ta, V, Nb and Mo) systems at 1650°C and in MgO-Fe alloy systems at 1550°C. In the SiO_2-refractory

metal systems, the metals reacted with SiO_2 to form metal oxides at the interface. The changes in the interfacial energies could not be determined due to the irregularities in the shape of the sessile drops. Similar oxide formation reactions were evident in the MgO-Fe alloy systems in vacuum. The dissociation of MgO, followed by the oxidation of iron, resulted in reduction of the liquid surface tension and the solid-liquid interfacial energy. Further reduction of the solid-liquid interfacial energy was observed in air when complete oxidation of Fe took place to form FeO. They pointed out that the system in vacuum was at pseudo-equilibrium since the oxidation of Fe was dependent upon other rate controlling steps. However, in air firing, the oxidation was rapid, and the true equilibrium state was attained immediately.

Kozakévitch[7] has shown that when a $CaO \cdot Al_2O_3 \cdot SiO_2$ slag is in contact with iron containing 0.7% sulfur at 1500°C, the interfacial energy drops from 800 ergs/cm^2 to less than 5 ergs/cm^2 and then increases back to 800 ergs/cm^2. He argued that this sudden drop of the interfacial energy was due to the diffusion of Fe^{2+} S^{2-} units (or couples) through the interface since the lowering of the interfacial energy due to a pure adsorption process could probably not account for such a drastic effect.

The effect of interface reactions on interfacial energy in the Cu-Al_2O_3 system has been studied by Chaklader, et al.[18] At 1230°C, with CuO additions to Cu, a decrease in the contact angle resulted due to $CuAlO_2$ formation at the interface. In air, complete wetting was obtained.

On metal-glass bonding, Pask and Fulrath[19] proposed a theory which states that chemical bonding at the interface occurs when there is a balance of bond energies across the transition zone between metal and

glass which occurs when the phases at the interface are saturated with the metal oxide. This concept was later discussed by Pask[20] in more detail. Pask and Borom[21] further pursued this theory on glass-metal bonding. They concluded that if the thermodynamic equilibrium does not exist at the interface, then a driving force exists for reactions at the interface to achieve such an equilibrium, the success of which is dependent upon the kinetics of the reactions. This analysis provides an explanation for the pseudoequilibrium conditions discussed by Armstrong, et al.[17]

B. Distribution of a Liquid Relative to Solids

The principles governing the spatial distribution of a liquid phase in a polyphase system were first established by Smith.[3] He showed that the spatial distribution of the liquid phase relative to solids depends only on the equilibrium dihedral angle. When $\phi<60°$, the liquid extends along the grain edges; when $\phi=0°$ the liquid extends along the grain faces; when $\phi>60°$ but $<120°$ the liquid is at the grain corners, and finally, when $\phi>120°$, there is no liquid present. The application of these principles in ceramic systems has been illustrated by Van Vlack[22] and White.[23]

In the SiO_2-iron oxide system Van Vlack[2] has shown that SiO_2 grains maintain a solid-solid contact at elevated temperatures and the oxidizing character of the atmosphere does not have any noticeable effect on the dihedral angle. The microstructure of magnesiowustite in the presence of a liquid phase containing MgO, FeO, and SiO_2 has also been studied by Van Vlack and Riegger.[24] Contrary to the SiO_2-iron oxide system, the degree of solid-solid contact was quite poor in this system. However, in the presence of a second solid phase, $FeAl_2O_4$, $FeFe_2O_4$, or $MgFe_2O_4$, the degree of contact between the grains improved. These spinel-type phases

formed bridges between the magnesiowustite grains, which they interpreted as a lower interfacial energy between unlike solid phases than that between two identical phases.

Riegger, et al.[25] have shown that in MgO-liquid systems, under the steel-making variables, a calcium silicate liquid penetrates between the periclase grains more than calcium ferrite and calcium aluminoferrite liquids. They have further suggested two factors for this contrast between the silicate liquids and the ferrite liquids: (a) a solid-liquid interfacial energy is low when the composition of the liquid is closer to that of the solid, and (b) adjustments at the boundaries in atomistic scale are more permissible in open atomic packing than in close atomic packing. The composition of silicate liquids is closer to that of periclase than the composition of ferrite liquids since the solubility of MgO is relatively high in the former liquids. Furthermore, the open framework of silicates would form a relatively low energy interface with the periclase grains. The formation of low energy grain boundaries between unlike grains was again observed in this study in the presence of a second solid phase.

Riegger, et al., and Van Vlack and Madden[26] have also studied the growth of solid phases in the above systems. They concluded that the presence of a second solid phase inhibits grain growth, and the growth is proportional to the square root of firing time.

Buist, et al.,[27] and Stephenson and White[28] have performed similar grain growth experiments in one solid+liquid and two solids+liquid systems. Grain growth was inhibited with the presence of a second solid phase which was in agreement with the observations of Riegger, et al.,

and Van Vlack and Madden. However, they found that the grain growth was proportional to the one third power of the firing time which differed from the former investigators' results.

A study of the factors controlling bonding in the periclase refractories has been performed by Jackson, et al.,[4] and Jackson and Ford.[5] In a periclase-monticellite system Cr_2O_3, Fe_2O_3, Al_2O_3, and TiO_2 were used as additives. It was concluded from these studies that among these additives only Cr_2O_3 additions increased the dihedral angle, promoted the degree of direct bonding between the solids, diminished the firing shrinkage, and inhibited grain growth of the periclase grains. Fe_2O_3, Al_2O_3, and TiO_2 additions were found to have a reverse effect on these properties. The appearance of a spinel phase was found to promote the degree of direct bonding since the spinel-periclase interfacial energy was low, and the spinel precipitates tended to form bridges between the periclase grains. Furthermore, as the CaO/SiO_2 ratio of the liquid was increased from 0.5 to 2.0 both the dihedral angle and the degree of solid-solid bonding increased.

C. Physical Properties in the Presence of a Liquid Phase

1. At Elevated Temperatures

The high temperature tensile strength of chrome-magnesite refractories has been investigated in the temperature range of 1290-1575°C by Ford, et al.[1] They showed that the tensile strength improved progressively as the extent of the direct bonding between the magnesite grains and between the chrome and magnesite increased. They also mentioned a temporary gap formation between the chrome and the periclase grains which could be due to either migration of the silicate liquid between the grains

at an intermediate stage or to the diffusion of iron oxide and chromic oxide from the chrome grain to the periclase.

Baker and Schroth[29] have reported that in chrome-magnesite and magnesia refractories the grain boundary spinel bond and the fused grain bond which is basically a spinel bond at the MgO solid-solid grain boundaries are the most effective ones for attaining high temperature strength.

In silica refractories the existence of a high strength at elevated temperatures has also been attributed, by Van Vlack,[2] to the formation of a solid skeleton between silica grains.

Kriek and Segal[30] have determined the high temperature strength of chrome-magnesite and magnesite refractories with torsion technique in the temperature range of 1300-1500°C. The lowest strength of the magnesite refractories corresponded to a CaO/SiO_2 ratio of 1.0. With a CaO/SiC_2 ratio of 2.0, the maximum strength was obtained which was higher than the strength of the direct bonded chrome-magnesite refractory. Thus, they concluded that in the achievement of high temperature strength the nature of the liquid phase is also as important as the direct bond formation of the chrome-magnesite refractories.

Hayhurst and Laming,[31,32] in heat treatment studies of the chrome-magnesite refractories, have shown that in the temperature range of 1500-1700°C the silicate liquid generally surrounds the solid grains. The direct bond which is observed at room temperature studies, therefore, is a result of precipitation during slow cooling in production. They observed that upon slow cooling, spinel and forsterite precipitated out between the periclase grains and formed an interlocked structure. The

observations of Konopicky[33] were also in agreement with these studies.

As indicated by Ford, et al. earlier, a gap containing a thin film of silicate was also observed by Hayhurst and Laming between a chrome grain and periclase envelope surrounding it. Recently, Brezny and Smutny[34] have shown that this gap, which hinders the direct bond formation, is due to the rapid diffusion of iron cations from chrome grains to periclase grains to achieve an equilibrium structure. They showed that by adding Fe_2O_3 into the periclase grains, thus reducing the iron concentration gradient between the chrome and the periclase grains, the rate of direct bond formation could be increased.

2. At Low Temperatures

In cermet systems, Humenik and Parikh,[35] and Parikh and Humenik[36] have shown that the presence of a continuous liquid film between the solid grains is desirable for achieving improved mechanical properties at low temperatures. A continuous liquid film which is undesirable at high temperatures was found to improve the hardness and impact resistance of titanium carbide base cermets upon solidification.

D. Sessile Drop Experiments in the MgO-Monticellite System

Raju and Pask[37] have recently initiated a program in order to understand the fundamental factors involved in the distribution of silicate liquids in multiphase magnesia and forsterite (Mg_2SiO_4) systems. As part of this program, they determined the contact angle of monticellite on (100) faces of MgO single crystals at 1550°C. The contact angle for the MgO-monticellite system was 45°. They have also investigated the effect of Cr_2O_3 and Fe_2O_3 additions to the liquid on the contact angle. Spreading of the liquid was observed with Cr_2O_3 additions in excess of 3%.

The contact angle decreased to a constant value of 15° with Fe_2O_3 additions in excess of 3%. It was proposed that in each case a reaction taking place at the interface could contribute to the lowering of the contact angle. The nature of these reactions, however, was not clearly understood.

III. EXPERIMENTAL PROCEDURE

The experimental procedure, in short, consisted of measuring the contact angles of premelted liquids on (100) faces of magnesium oxide single crystals and then studying the polished cross sections of the interface with an optical microscope and an electron microprobe analyzer.

The liquids were prepared with reagent grade MgO, $CaCO_3$, SiO_2 and additive oxide Al_2O_3, Cr_2O_3, Fe_2O_3, and TiO_2 powders. The chemical analyses of these powders are given in the appendix. The batches were dry mixed and melted in platinum crucibles in air, at temperatures approximately 25-75° higher than the subsequent test temperature.

The magnesium oxide single crystals were obtained from the Muscle Shoals Electrochemical Corporation.* The spectrographic analysis of an average sample is given in the appendix. Substrates of approximately 1/2" x 1/2" and 1/8" thick were cleaved from approximately 1" x 1" x 1" single crystal boules. First, these substrates were polished in boiling H_3PO_4 acid before the sessile drop experiments. Later this step was omitted since the same results could be obtained with experiments repeated on freshly cleaved substrates cleaned with ethanol.

Two types of furnaces were used: (a) a gas/air fired Bickley model 2150 furnace, for temperatures higher than 1550°C, and (b) a quench type furnace with $MoSi_2$ heating elements. The Bickley furnace was monitored and controlled by a Honeywell-Radiamatic recorder-controller. The quench furnace was monitored and controlled by a Leeds and Northrup Speedomax-H recorder-controller. A sketch of the quench furnace has been given by Blank.[33]

*P.O. Box 87, Tuscumbia, Alabama

The sessile drop experiments were performed at 1550°C in air. Some experiments, which will be discussed in the following sections, were performed at 1700°C. A small piece of premelted liquid was placed on a MgO single crystal which was covered with either a platinum or magnesia crucible to prevent any contamination from the furnace. The specimens were held at the test temperature for approximately 3 hours. Firings for shorter (1 hour) or longer (up to 5 hours) periods did not alter the results. Subsequently, the power was shut off, and the specimens were cooled in the furnace.

Contact angles were measured at room temperature using a telescope equipped with a filar-micrometer eyepiece. This apparatus has been described by Brennan.[39] The specimens were then cut with a diamond saw perpendicular to the interface, polished, and were subjected to metallographic examination. The polishing was done on 1, 1/0, 2/0 and 3/0 emery papers followed with a short polishing step with 0.3μ Al_2O_3 on a lap.

The electron microprobe* analyses were done on the same specimens. Carbon was vacuum-deposited, and the portions around the interface were coated with a slurry of carbon in ethanol in order to improve the surface conductivity. The areas of interest were scanned with an electron beam of 20KV and a specimen current of approximately 0.03μA, and the excited Kα x-radiations were counted with spectrometers. The oscilloscope traces of the relative intensities were then used to analyze the specimens semi-quantitatively.

---

*Analyzer was a Materials Analysis Company model 400 type.

IV. RESULTS AND DISCUSSION

A. Contact Angle Measurements

The results of the sessile drop experiments which show the effect of Al_2O_3, Cr_2O_3, Fe_2O_3, and TiO_2 additions to monticellite at 1550°C are shown in Fig. 2. The measurements which are indicated with solid marks are those of Raju and Pask.[37] The contact angle of the monticellite liquid without any additions on MgO was found to be in the range of 43-51°. A photomicrograph of the cross section of a typical monticellite-periclase interface is shown in Fig. 3. The average 47° angle of the monticellite-periclase system decreased to a constant value of 35° with addition of more than 5% Al_2O_3 to the liquid. The decrease of contact angle was more pronounced with Fe_2O_3 (15°) and Cr_2O_3 (0°, spreading) additions. Again, the angles became constant after about 3% R_2O_3 addition. Spreading was observed with 30% TiO_2 addition although the sample with 5% TiO_2 had a contact angle of 16°.

Table I. Wetting of MgO by Cr_2O_3 Containing Silicate Liquids

Drop Composition	Test Temp. (°C)	Time at Temp. (hrs.)	Contact Angle
4% $MgCr_2O_4$ + 96% $CaO{\cdot}MgO{\cdot}SiO_2$	1550	3	16-18°
" "	1700	4	15°
20% Cr_2O_3 + 40% MgO + 40% $CaO{\cdot}SiO_2$	1700	3	Spreading

In Table I, the results of the experiments with Cr_2O_3 containing liquid compositions other than the ones shown in Fig. 2 are given. The

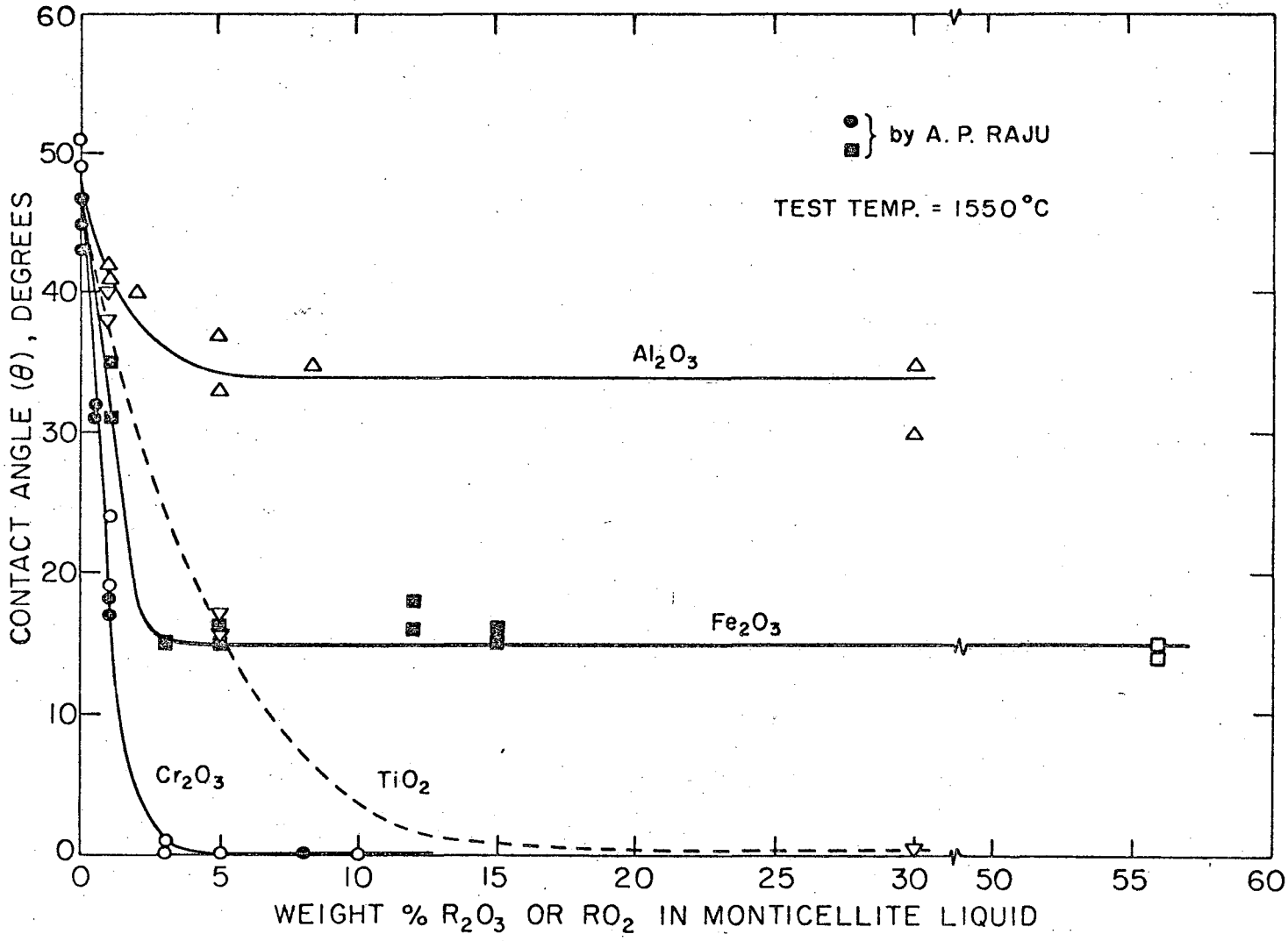

XBL 6810-6024

Fig. 2. Effect of R_2O_3 and TiO_2 additions to monticellite on contact angle after 3 hours at 1550°C.

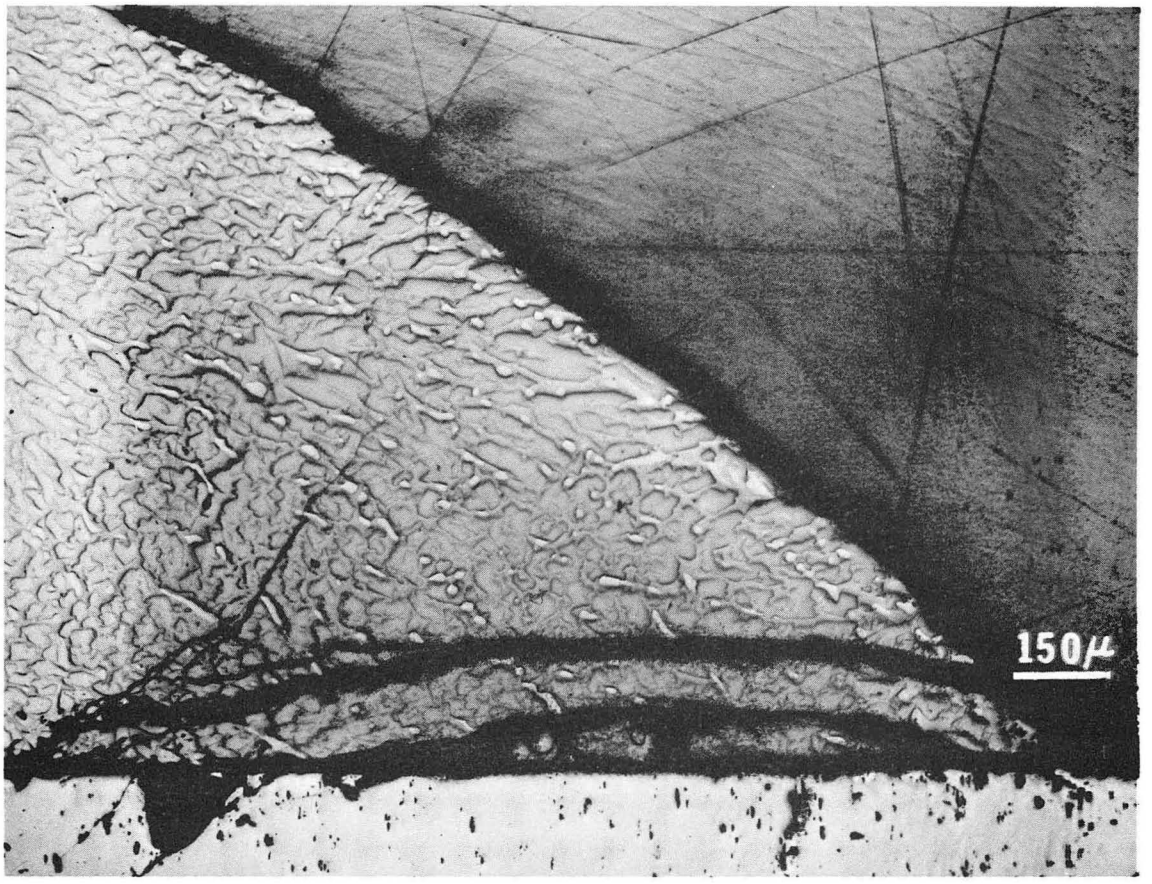

XBB 6810-6116

Fig. 3 Photomicrograph of the cross section of a monticellite sessile drop on magnesium oxide, held 3 hours at 1550°C.

experiment with 4% $MgCr_2O_4$ addition to the monticellite was performed both at 1550° and 1700°C which showed finite contact angles of 16-18° and 15°, respectively. The experiments with 20% Cr_2O_3, however, could only be performed at 1700°C since a minute amount of liquid formed below this temperature. Spreading was observed in this latter experiment.

In sessile drop experiments the adsorption of additives either at the solid-liquid interface or the liquid surface has an important effect on the equilibrium value of the contact angle. The observations of Halden and Kingery,[8] and Kingery[14] on the liquid iron-Al_2O_3 system when S, O, N, or C adsorbed at the surface and when Si adsorbed at the interface were good illustrations of the adsorption phenomenon. Similarly, Kurkjian and Kingery[9] illustrated the effect of adsorption on the contact angle in the liquid nickel-Al_2O_3 system when Sn and In adsorbed at the surface and Cr and Ti adsorbed at the interface.

On the other hand, if the liquid drop and the solid are not at a thermodynamic equilibrium, a redistribution of the components between the liquid and the solid will take place. An equilibrium contact angle will form only after this thermodynamic equilibrium is achieved. The phenomena which would occur during this transient redistribution or the reaction stage, however, are not clearly understood. In metal-ceramic systems, the wetting tendency increased whenever interfacial reactions occurred, according to Humenik and Kingery.[13] They concluded that this increase in the wetting tendency was due to a decrease in the interfacial energy caused by a composition change at the interface. The lowering of the interfacial energy in the metal-ceramic systems studied by Armstrong, et al.,[15,17] and Chaklader, et al.[18] was attributed to the formation of a

stable phase at the interface. Finally, the drastic drop observed by Kozakévitch[7] in the interfacial energy of the $CaO \cdot Al_2O_3 \cdot SiO_2$-iron system was attributed to the diffusion of Fe^{2+} S^{2-} units through the interface.

In the monticellite-periclase system of this investigation, monticellite itself is at a chemical equilibrium with MgO at 1550°C, by a slight precipitation of MgO in the liquid, according to the phase diagram drawn by Osborn and Muan.[40a] However, with the addition of Al_2O_3, Cr_2O_3, Fe_2O_3, and TiO_2, this equilibrium will be disturbed, and the liquid and the substrate will react to attain a thermodynamic equilibrium. An examination of the equilibrium phase diagrams corresponding to these systems will lead to the understanding of the nature of these reactions.

B. Phase Diagrams

In the literature, sufficient data were available to construct the equilibrium phase diagrams of the R_2O_3-MgO-$CaO \cdot SiO_2$ systems. The work of the author was merely to make use of these data in order to draw the diagrams presented in the following sections.

1. The Al_2O_3-MgO-$CaO \cdot SiO_2$ System

The Al_2O_3-MgO-$CaO \cdot SiO_2$ equilibrium diagram is shown in Fig. 4. The details of the MgO-Al_2O_3 joint of this system are from the work of Roy, et al.,[42] and of Alper, et al.[43] The details of the MgO-$CaO \cdot SiO_2$ joint and the Al_2O_3-$CaO \cdot SiO_2$ edge are from the diagrams drawn by Osborn and Muan.[40a,40b] On the MgO-$CaO \cdot SiO_2$ joint the compounds $CaO \cdot MgO \cdot SiO_2$ and $2CaO \cdot MgO \cdot 2SiO_2$ are represented as CMS and C_2MS_2, respectively. El-Shahat and White[44] have recently worked on the $MgO \cdot Al_2O_3$-CMS joint, and their results have been found to be essentially in agreement with an earlier work by Osborn, et al.[45] This latter work was used to complete the rest

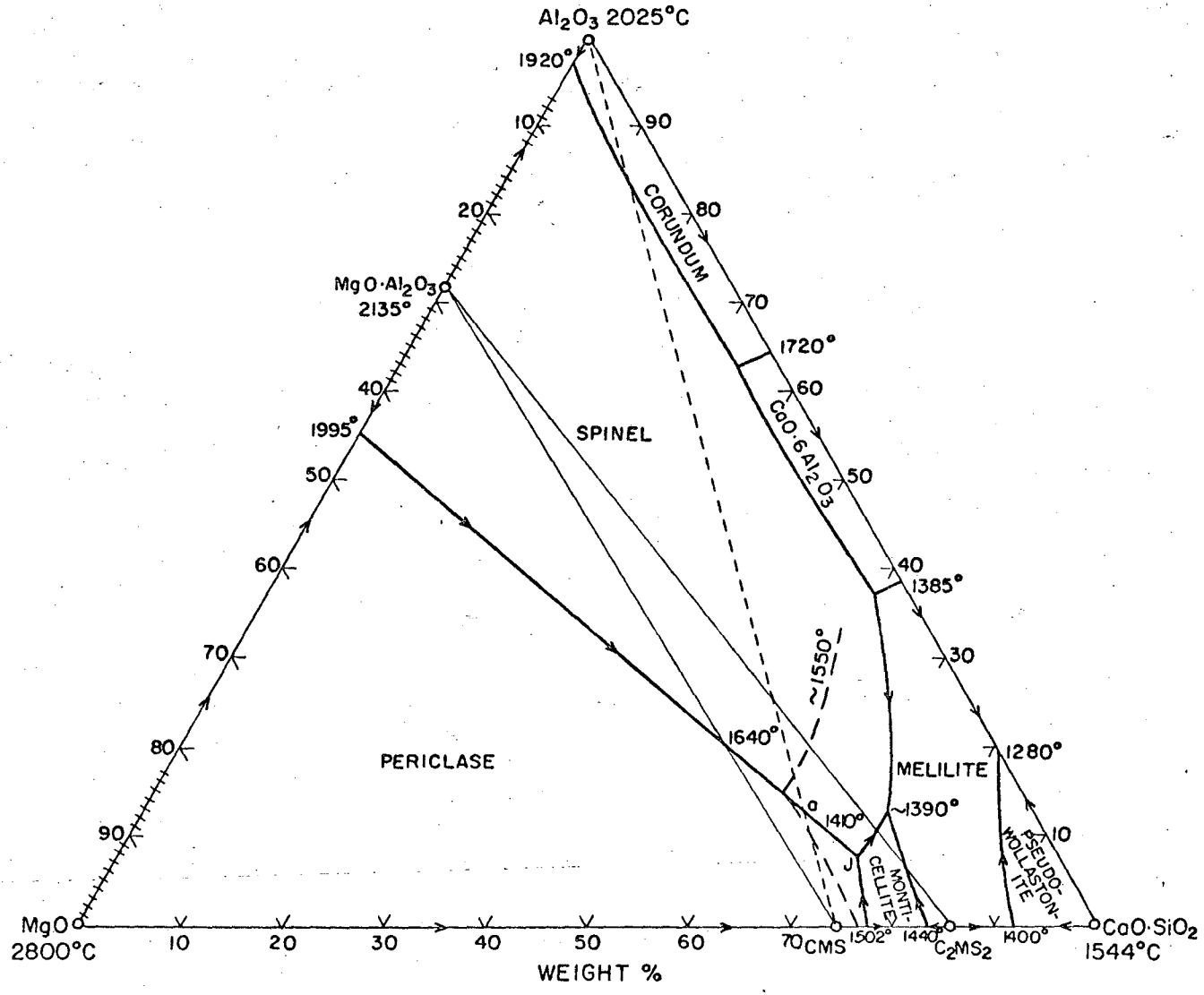

XBL 6810-6031

Fig. 4. Al_2O_3-MgO-$CaO \cdot SiO_2$ equilibrium phase diagram.

of the diagram.

The overall compositions of the drops used in this study varied along the dash line connecting Al_2O_3 to CMS. An approximate 1550°C isotherm is shown with long dash lines in the spinel and periclase primary fields. When additions of up to 10% Al_2O_3 are made to CMS at 1550°C, the liquid is at equilibrium not with pure MgO, but with a MgO-Al_2O_3 solid solution. Thus, when this liquid is in contact with a MgO substrate, it will react with the substrate to form an equilibrium solid solution structure. With additions in excess of 10% Al_2O_3, the liquid becomes deficient in MgO. The liquid will then dissolve MgO from the substrate to reach an equilibrium composition along the 1550°C isotherm. If the Al_2O_3 content of the drop is high enough to saturate the liquid with respect to $MgO \cdot Al_2O_3$ (spinel), the nature of the interface reactions becomes more complicated since the liquid might now also react with the substrate to form spinel. During cooling, the liquid drop probably behaves independently due to fairly rapid cooling rates (~50° C/min.). After passing through the peritectic point "J", the last portion of the liquid should freeze at the eutectic point, at 1390°C, where only the spinel, monticellite, and melilite phases would be present under equilibrium conditions.

2. The Cr_2O_3-MgO-$CaO \cdot SiO_2$ System

The Cr_2O_3-MgO-$CaO \cdot SiO_2$ equilibrium diagram is shown in Fig. 5. The MgO-Cr_2O_3 joint of this system has been determined by Alper, et al.,[46] and Wilde and Rees.[47] The Cr_2O_3-$CaO \cdot SiO_2$ edge is from the work of Glasser and Osborn.[48] El-Shahat and White's[44] work on the $MgO \cdot Cr_2O_3$-$CaO \cdot MgO \cdot SiO_2$ joint has provided all the information needed for this study. Although Ford and Rees[40c] showed that $MgO \cdot Cr_2O_3$ joins to both

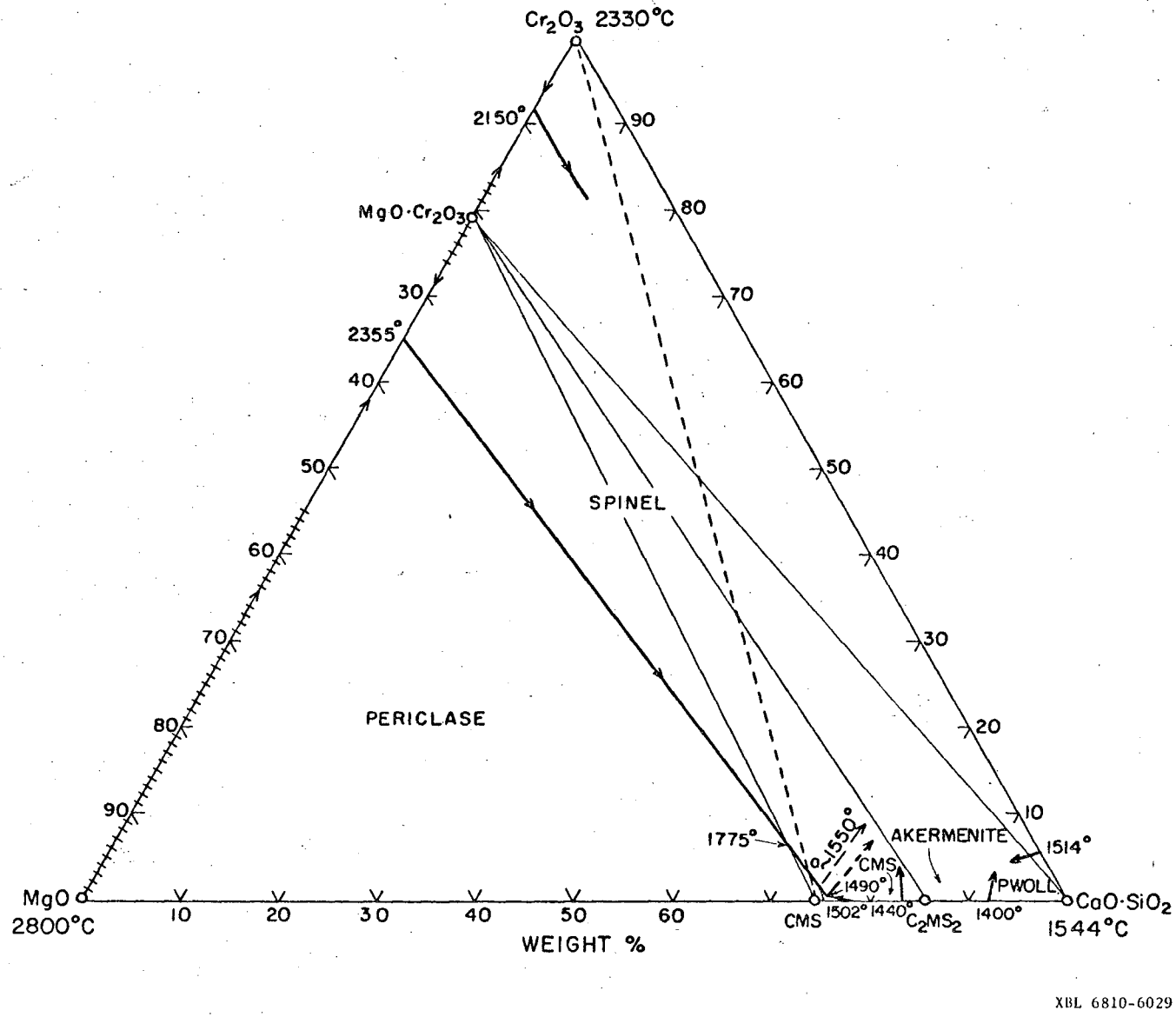

Fig. 5. Cr_2O_3-MgO-$CaO \cdot SiO_2$ equilibrium phase diagram.

$2CaO \cdot MgO \cdot 2SiO_2$ and $CaO \cdot SiO_2$, the details of the rest of the diagram still remain to be determined. Again, the behavior of the liquid and the nature of the reactions between the liquid and the substrate are the same as those in the Al_2O_3-MgO-$CaO \cdot SiO_2$ system. The main difference is that here only a small amount of Cr_2O_3 is needed to saturate the liquid with respect to $MgO \cdot Cr_2O_3$.

3. The Fe_2O_3-FeO-MgO-$CaO \cdot SiO_2$ System

The Fe_2O_3-MgO-$CaO \cdot SiO_2$ system is somewhat more complicated than the former ones since, with the loss of oxygen, Fe_2O_3 dissociates in the FeO direction. In this case, therefore, one actually deals with a quaternary system. An attempt has been made to draw this system as shown in Fig. 6 after an original quaternary drawing of El-Shahat and White.[44] The MgO-Fe_2O_3-FeO section of the diagram is from a recent work of Willshee and White.[49] The $MgFe_2O_4$-CMS joint has been investigated by El-Shahat and White. Although Berezhnoi[40d] has determined that $MgFe_2O_4$ joins to both $2CaO \cdot MgO \cdot 2SiO_2$ and $CaO \cdot SiO_2$, the details of these joints have yet to be determined.

In this system, for example, any composition along the dash line between Fe_2O_3 and CMS at room temperature will correspond to some other composition at high temperatures in the plane outlined by the dash lines and Fe_2O_3-FeO axis. The liquid at point "a" will be at equilibrium with a magnesiowustite solid solution as given by the upper border of the MgO-D magnesiowustite solid solution field. It will also be at equilibrium with a $MgFe_2O_4$ spinel solid solution as given by the line $MgFe_2O_4$-E-Fe_3O_4. The liquids corresponding to a point on the liquidus passing through MgO, L, a, and J will be at equilibrium only with a magnesio-

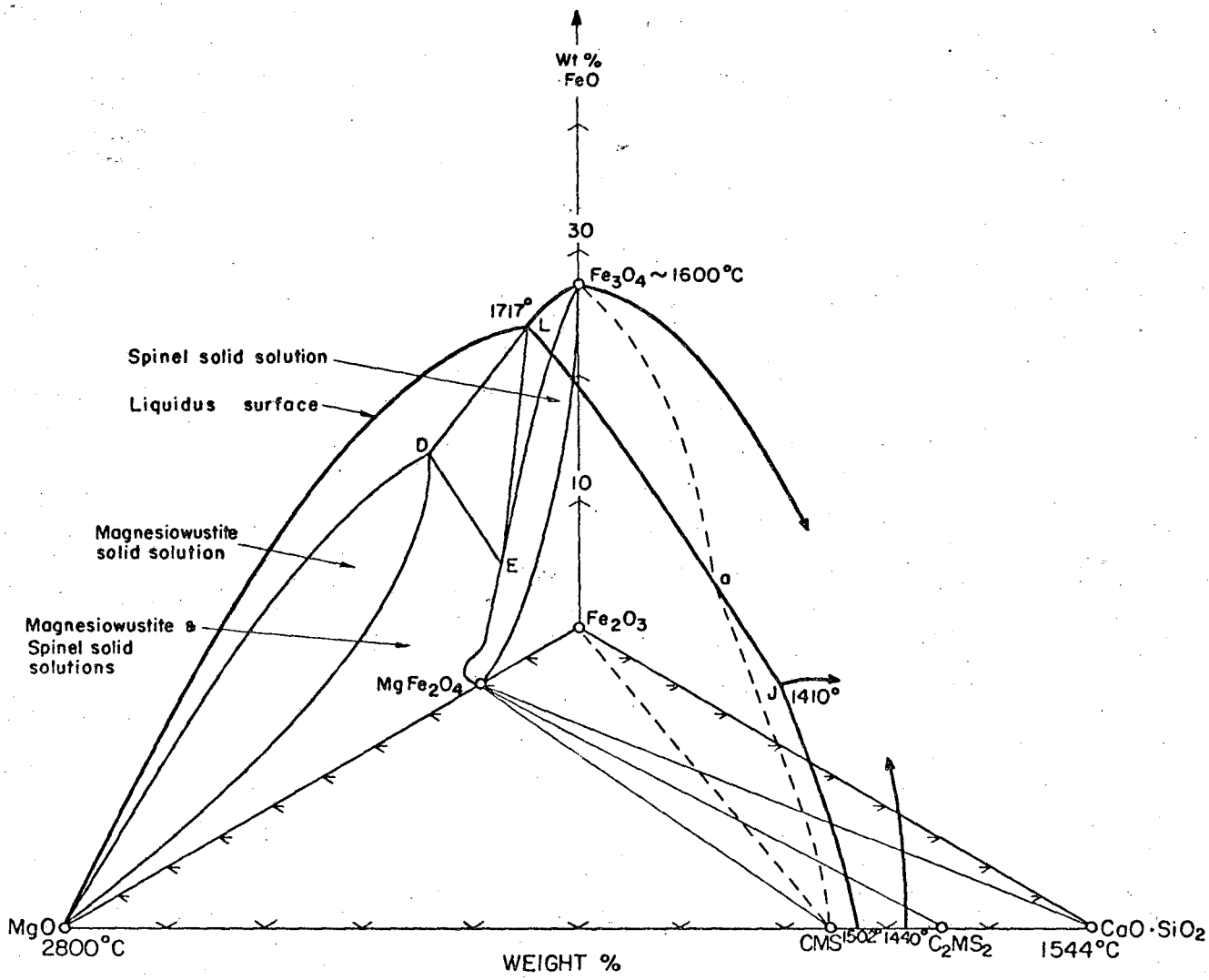

Fig. 6. Fe_2O_3-FeO-MgO-$CaO \cdot SiO_2$ equilibrium phase diagram.

wustite solid solution. The liquidus passing through Fe_3O_4, L, a, and J will contain liquids which will be at equilibrium only with a spinel solid solution. The behavior of the liquid drops on MgO and the nature of the interface reactions will again be similar to those of the previous systems.

4. The $MgO-R_2O_3$ Solid Solutions

In Fig. 7, the $MgO-R_2O_3$ solid solution portions of the $MgO-R_2O_3$ binary systems are superimposed for a direct comparison of the solid solubility limits. The $MgO-Al_2O_3$ and $MgO-Cr_2O_3$ sections are from the diagrams drawn by Alper, et al.,[43,46] and the $MgO-Fe_2O_3$ section is from the diagram drawn by Willshee and White.[49] At elevated temperatures, the $MgO-Fe_2O_3$ system indicated here is not a binary system but a projection of the $MgO-Fe_2O_3-FeO$ ternary system on the $MgO-Fe_2O_3$ axis. At 1550°C, the solid solubility limits are 9% and 50% of Cr_2O_3 and $Fe_2O_3(-FeO)$, respectively, and almost 0% of Al_2O_3 in MgO. Thus, at this temperature, when a drop containing Fe_2O_3 is placed on a MgO substrate, most of the iron will diffuse into the MgO. Since the mass of the drop is smaller than that of the substrate, the drop will never have enough iron to saturate both the liquid and the substrate. At equilibrium the system will always be undersaturated. However, with Al_2O_3 and Cr_2O_3 additions, one could expect to attain the saturation of the whole system if enough R_2O_3 is added to the liquid initially.

5. The $TiO_2-MgO-CaO\cdot SiO_2$ System

Sufficient data are not available in the literature to construct a ternary diagram similar to those given above. According to Berezhnoi,[40e]

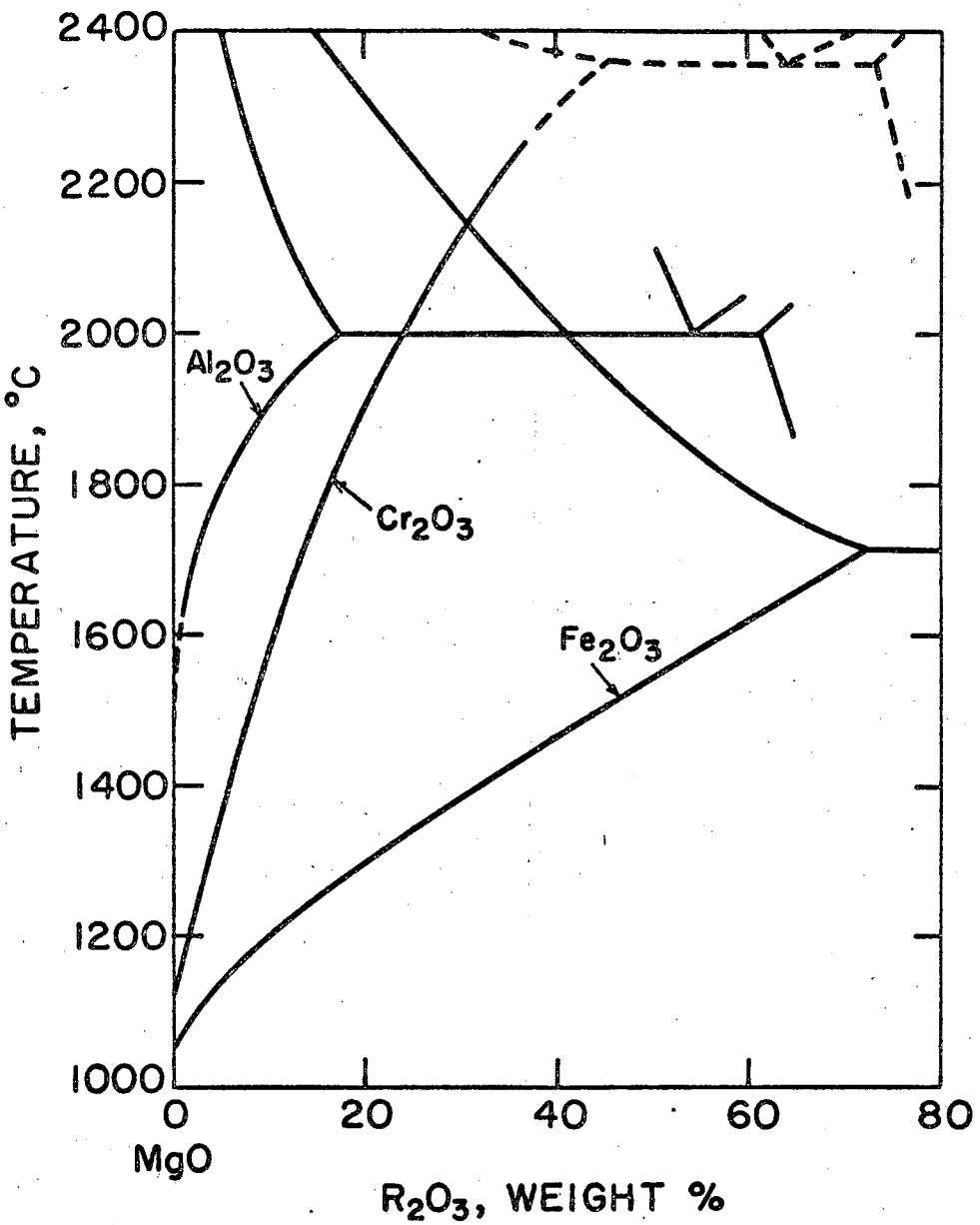

XBL 6810-6026

Fig. 7. $MgO-R_2O_3$ solid solution regions of the $MgO-MgCr_2O_4$, $MgO-MgAl_2O_4$, and $MgO-MgFe_2O_4$ systems.

with 5% TiO_2 addition to $CaO \cdot MgO \cdot SiO_2$, the overall drop composition would be inside the $CaO \cdot TiO_2$-$2CaO \cdot MgO \cdot 2SiO_2$-$CaO \cdot MgO \cdot SiO_2$-$2MgO \cdot SiO_2$ composition tetrahedron. Thus, any of these solids can coexist in equilibrium with the liquid portion of the drop. Due to the incongruent melting of $CaO \cdot MgO \cdot SiO_2$ one would expect the MgO primary field to extend into this composition tetrahedron. Then, at temperatures above the peritectic reaction temperature, MgO can also coexist in equilibrium with the liquid. The peritectic temperature of the MgO-CMS system is 1502°C (Fig. 4). This temperature would be lowered below 1502°C when TiO_2 is added to the system. Therefore, since the 1550°C test temperature of this investigation would be above the peritectic temperature, any liquid placed on the MgO substrate would either be in or at the boundary of the MgO primary field after equilibrium is achieved. If the liquid composition is outside this primary field initially, it will dissolve MgO from the substrate surface to attain this equilibrium composition. With 30% TiO_2 addition to $CaO \cdot MgO \cdot SiO_2$, the first liquid to form would definitely be outside the MgO primary field since the overall drop composition is now in another composition tetrahedron, and the MgO primary field would not extend into this tetrahedron. According to Berezhnoi's diagram, this new composition tetrahedron would be $CaO \cdot TiO_2$-$CaO \cdot MgO \cdot 2SiO_2$-$2CaO \cdot MgO \cdot 2SiO_2$-$2MgO \cdot SiO_2$.

TiO_2 and MgO react to form the compounds $2MgO \cdot TiO_2$, $MgO \cdot TiO_2$, and $MgO \cdot 2TiO_2$ as shown in the MgO-TiO_2 equilibrium phase diagrams of Massazza and Sirchia,[40f] and Coughanour and DeProsse.[40g] No solid solution of TiO_2 in MgO is indicated in these diagrams. Alper[41] points out that Ti^{4+}, which is the stable state in an air atmosphere, is very insoluble

in MgO even at high temperatures. Thus, only a neglible amount of TiO_2 in the liquid may react with the substrate to form a solid solution. Furthermore, at the liquid-solid interface, there would be no compound formation since the primary fields of the compounds indicated above are not in the composition tetrahedrons.[40e]

C. Optical Microscope and Electron Microprobe Studies

The optical microscope and electron microprobe studies were in agreement with the equilibrium diagrams presented in the previous section. Although all of the samples were examined, only the typical examples of various combinations will be discussed to avoid repetition.

1. Al_2O_3-MgO-CaO·SiO_2 System

In Fig. 8, the interface of the sample with an original drop composition of 1% Al_2O_3 + 99% CMS is shown. At 1550°C, the liquid portion of the drop is in the MgO primary field. Thus, the only interaction between the liquid and the substrate is the formation of MgO-Al_2O_3 solid solution at the interface. According to the equilibrium phase diagram, at room temperature the drop will contain spinel, monticellite, and melilite but no periclase. However, since the cooling rates are fast, a non-equilibrium structure is frozen in. The oscilloscope trace of the same sample is shown in Fig. 9 where the white areas indicate the presence of the corresponding element. In the liquid only the MgO particles containing a high magnesium concentration and some aluminum in solid solution can be identified distinctly. The MgO which constitutes the solid portion of the drop was present in the liquid at 1550°C (light color, round particles, in Fig. 8), whereas the remaining dendrites formed during cooling. Some segregation is observed in the matrix due to the precipitation

in MgO even at high temperatures. Thus, only a neglible amount of TiO_2 in the liquid may react with the substrate to form a solid solution. Furthermore, at the liquid-solid interface, there would be no compound formation since the primary fields of the compounds indicated above are not in the composition tetrahedrons.[40e]

C. Optical Microscope and Electron Microprobe Studies

The optical microscope and electron microprobe studies were in agreement with the equilibrium diagrams presented in the previous section. Although all of the samples were examined, only the typical examples of various combinations will be discussed to avoid repetition.

1. Al_2O_3-MgO-CaO·SiO_2 System

In Fig. 8, the interface of the sample with an original drop composition of 1% Al_2O_3 + 99% CMS is shown. At 1550°C, the liquid portion of the drop is in the MgO primary field. Thus, the only interaction between the liquid and the substrate is the formation of MgO-Al_2O_3 solid solution at the interface. According to the equilibrium phase diagram, at room temperature the drop will contain spinel, monticellite, and melilite but no periclase. However, since the cooling rates are fast, a non-equilibrium structure is frozen in. The oscilloscope trace of the same sample is shown in Fig. 9 where the white areas indicate the presence of the corresponding element. In the liquid only the MgO particles containing a high magnesium concentration and some aluminum in solid solution can be identified distinctly. The MgO which constitutes the solid portion of the drop was present in the liquid at 1550°C (light color, round particles, in Fig. 8), whereas the remaining dendrites formed during cooling. Some segregation is observed in the matrix due to the precipitation

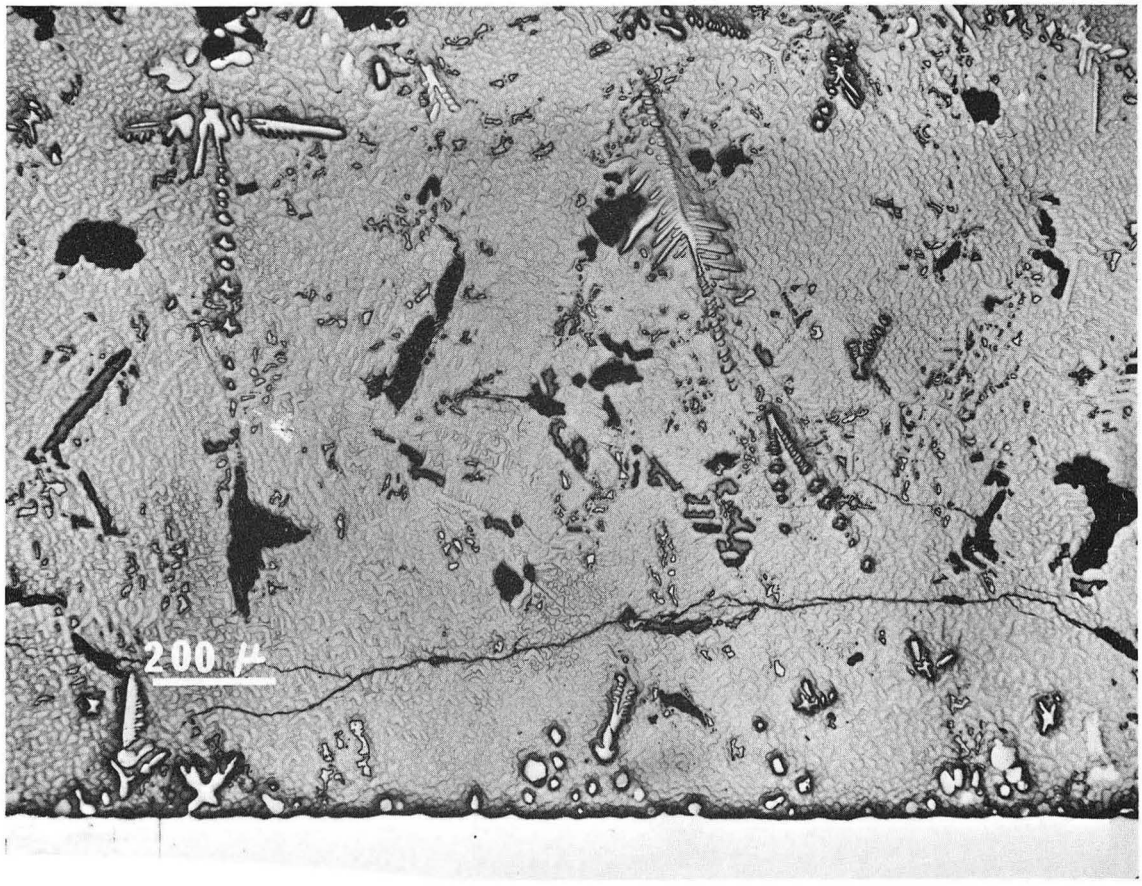

XBB 6810-6113

Fig. 8 Solid-liquid interface of the sample with an original drop composition of 1% Al_2O_3 + 99% CMS, held 3 hours at 1550°C.

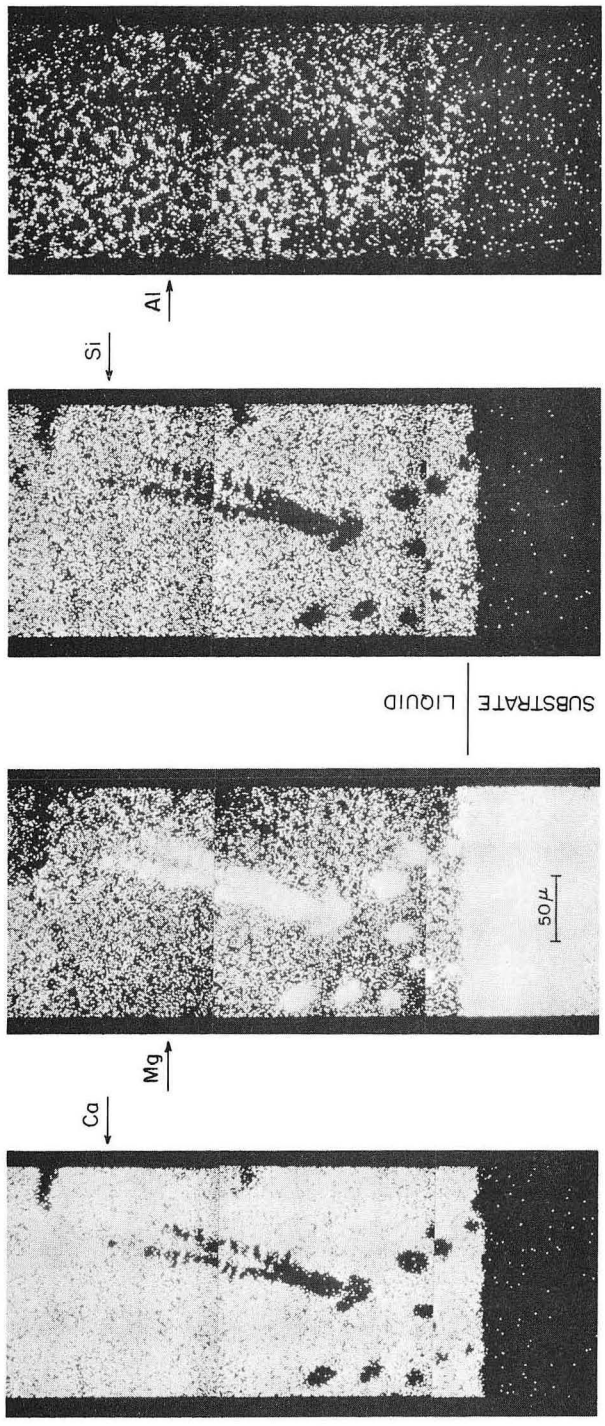

XBL 6810-6097

Fig. 9 Oscilloscope trace of the solid-liquid interface of the sample with an original drop composition of 1% Al_2O_3 + 99% CMS, held 3 hours at 1550°C.

of monticellite and spinel. The voids in the drop appear as the dark areas in Fig. 8. In the MgO substrate some aluminum could be detected, although most of it was due to the background.

2. Cr_2O_3-MgO-CaO·SiO_2 System

The liquid-solid interface of the sample containing an original liquid composition of 4% $MgCr_2O_4$ + 96% CMS is shown in Fig. 10. The structure of the drop observed at room temperature is not the equilibrium structure of spinel, monticellite, and akermenite, but a non-equilibrium structure of a frozen-in matrix containing MgO solid solution particles, similar to the previous sample. The liquid of this sample at 1700°C contains only particles of MgO with Cr_2O_3 in solid solution. These particles appear as the light gray, round particles. The oscilloscope trace of this same sample, shown in Fig. 11, verifies the existence of chromium in those particles which showed a high magnesium concentration with some chromium. The matrix shows a very low chromium concentration. As shown in Fig. 7, the maximum solubility of Cr_2O_3 in MgO at 1700°C is about 13%. Thus the liquid will be losing some of its chromium to the substrate. In Fig. 11, the diffusion layer of chromium in the substrate appears to be about 60μ.

3. Fe_2O_3-MgO-CaO·SiO_2 System

The experiment with an original drop composition of 56% Fe_2O_3 + 44% CMS illustrates a case in which the premelted liquid is not at equilibrium with MgO but is at equilibrium with spinel. At 1550°C, the liquid portion of this drop will correspond to a composition on the liquidus surface passing through Fe_3O_4, L, a, and J, in Fig. 6. The solid portion of the drop will be a $MgFe_2O_4$-Fe_3O_4 solid solution. When this drop is in

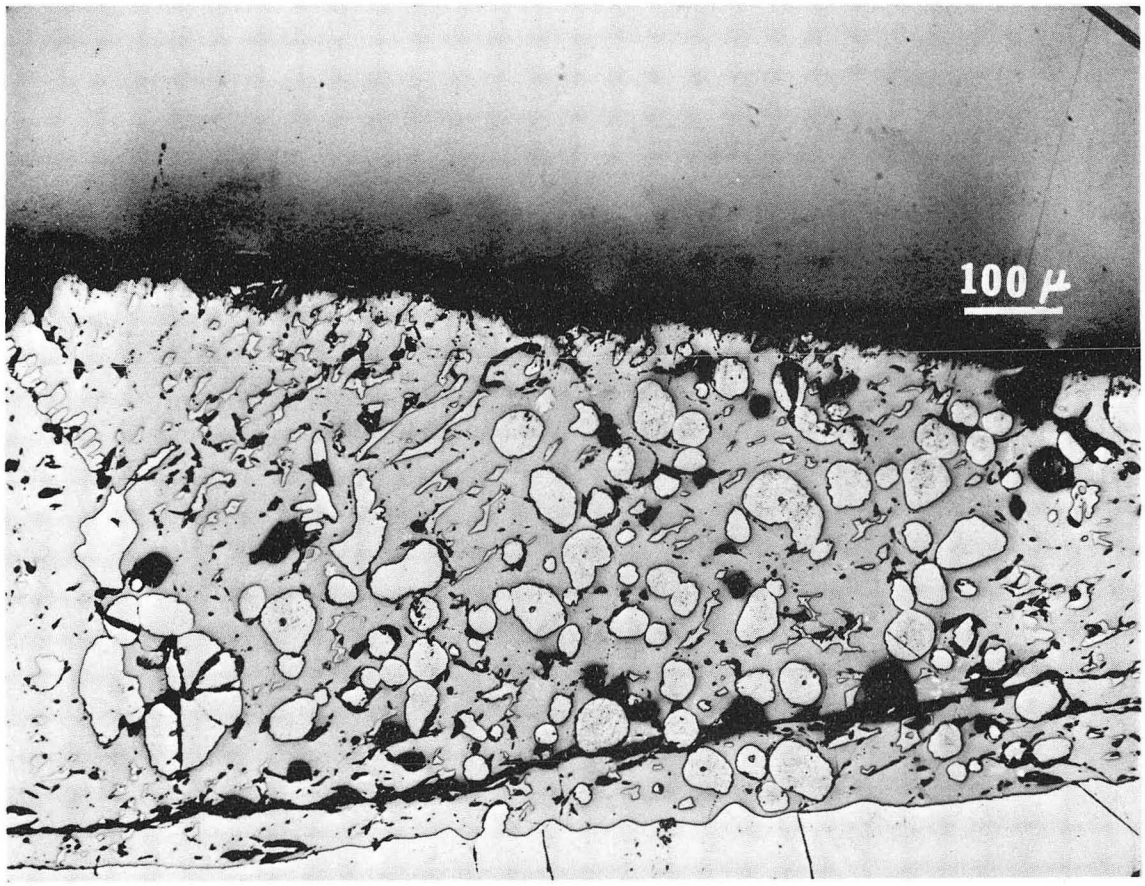

XBB 6810-6123

Fig. 10 Solid-liquid interface of the sample with an original drop composition of 4% $MgCr_2O_4$ + 96% CMS, held 4 hours at 1700°C.

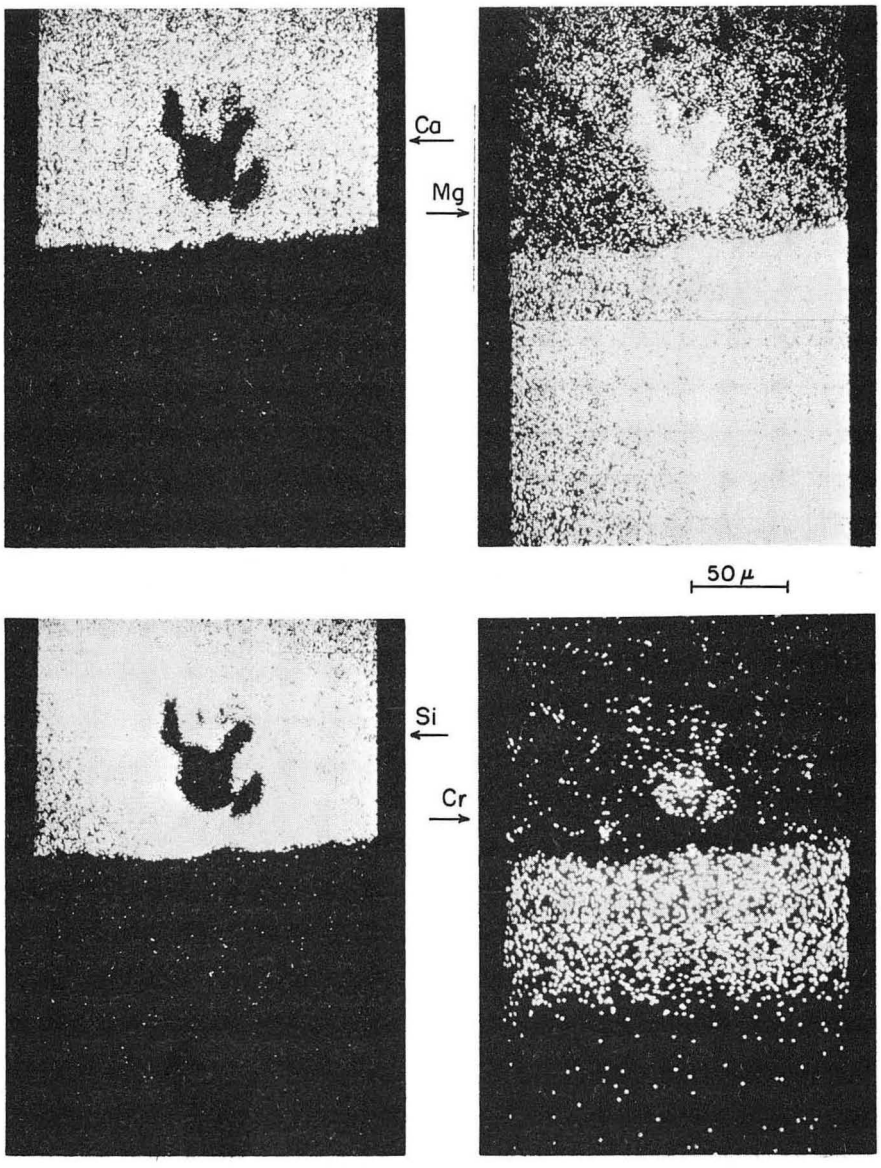

Fig. 11 Oscilloscope trace of the solid-liquid interface of the sample with an original drop composition of 4% $MgCr_2O_4$ + 96% CMS, held 4 hours at 1700°C.

contact with a MgO substrate, the substrate can react with the liquid at the interface to form either a spinel or a magnesiowustite solid solution. At the same time the liquid will dissolve MgO from the surface to reach equilibrium with the substrate. As a result, the liquid composition will shift towards the "LaJ" boundary line. During cooling, the liquid will follow this boundary line, while both magnesiowustite and spinel will precipitate out. All the magnesiowustite in the liquid should disappear at the peritectic point "J" before the liquid moves along the monticellite-spinel boundary line. However, since the cooling rates are fast, some magnesiowustite will also be seen at room temperature.

A photomicrograph of the liquid-solid interface of this sample is shown in Fig. 12. In the liquid drop, the angular white particles are the $MgFe_2O_4$ solid solution while the round gray ones containing small spinel particles are the magnesiowustite solid solution. Some spinel apparently precipitates out during cooling inside the magnesiowustite particles. The remaining portion of the drop is primarily monticellite (dark gray) and the final portion of the liquid which freezes at the invariant point. An iron diffusion layer of about 400μ is also apparent in the Fe-Kα trace.

4. TiO_2-MgO-$CaO \cdot SiO_2$ System

As indicated in the discussion of the TiO_2-MgO-$CaO \cdot SiO_2$ system, with additions of TiO_2 the liquid dissolves MgO from the substrate to reach saturation with respect to MgO. Only a very small amount of TiO_2 in the liquid may react with the substrate to form a solid solution, while no compound formation at the interface will take place. With 5% TiO_2 addition any of the solids, $CaO \cdot TiO_2$, $2CaO \cdot MgO \cdot 2SiO_2$, $CaO \cdot MgO \cdot SiO_2$,

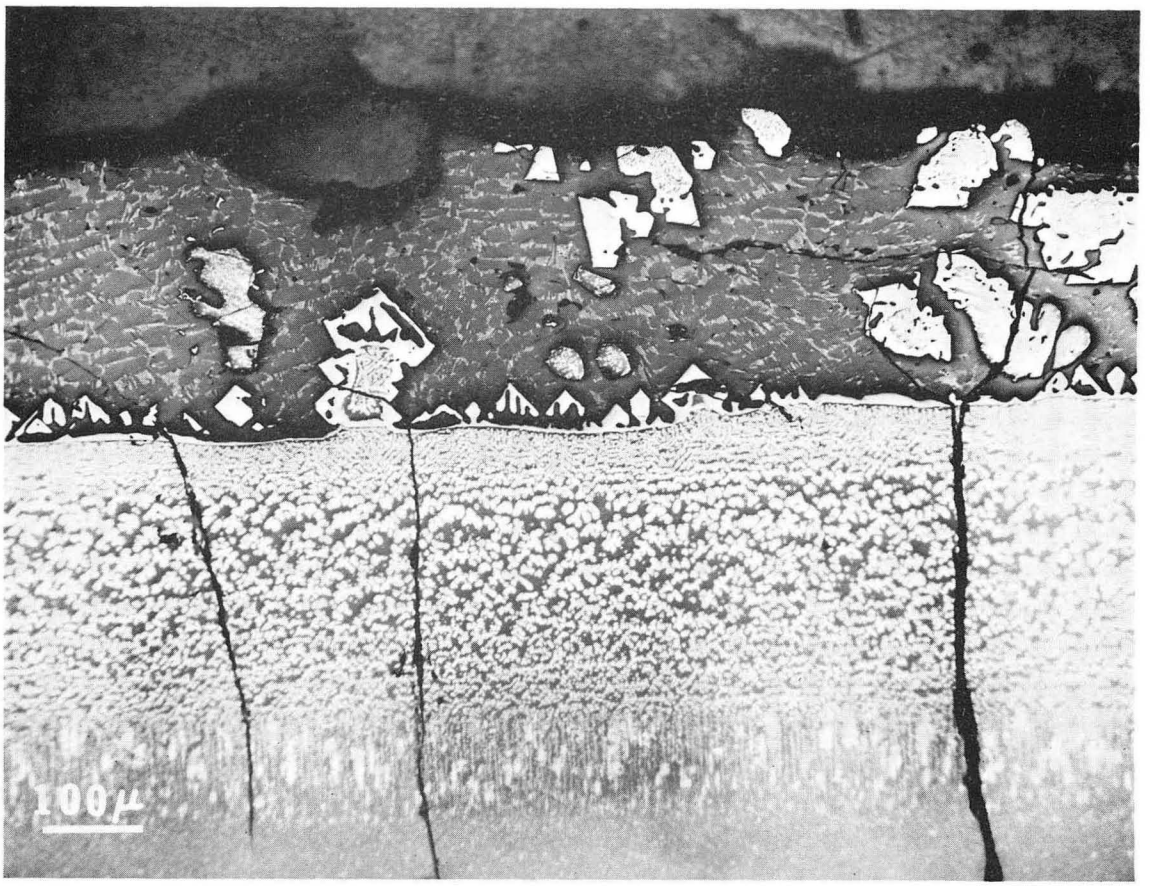

XBB 6810-6105

Fig. 12 Solid-liquid interface of the sample with an original drop composition of 56% Fe_2O_3 + 44% CMS, held 3 hours at 1550°C.

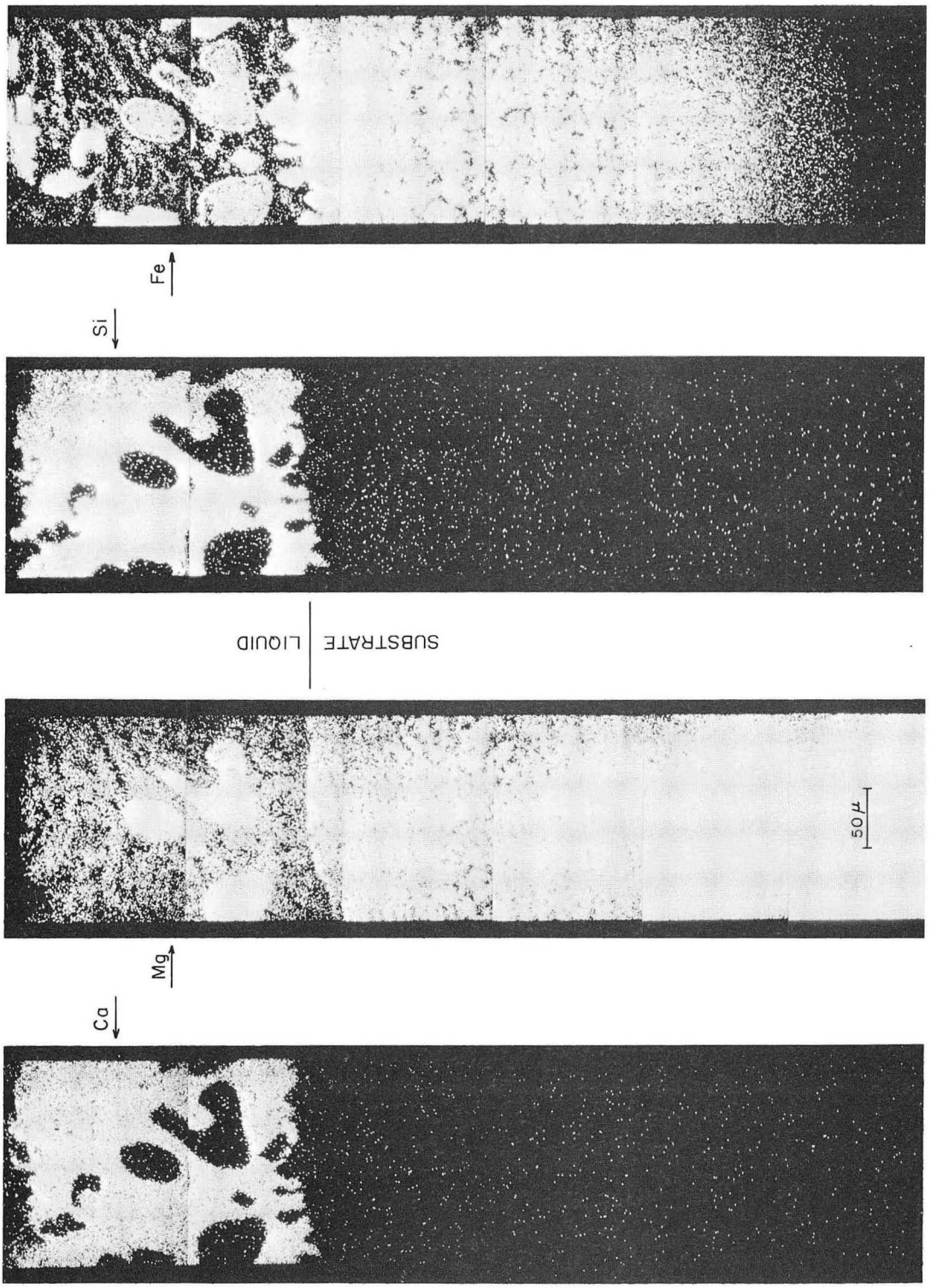

XBL 6810-6098

Fig. 13 Oscilloscope trace of the solid-liquid interface of the sample with an original drop composition of 56% Fe_2O_3 + 44% CMS, held 3 hours at 1550°C.

$2MgO \cdot SiO_2$, and MgO can be expected to coexist with the liquid. With 30% TiO_2 addition, $CaO \cdot MgO \cdot 2SiO_2$ replaces $CaO \cdot MgO \cdot SiO_2$. In Fig. 14 a photomicrograph of the sample with 5% TiO_2 containing liquid is shown. A comparison of this micrograph with the oscilloscope traces of the elements given in Fig. 16(a) shows that the white angular particles in the liquid contain only calcium and titanium. Thus, the white particles correspond to the $CaO \cdot TiO_2$ phase. The light gray, round particles concentrated close to the liquid-solid interface indicate only the presence of magnesium, and thus, they will be the MgO phase. The dark gray sections, which constitute the main portion of the liquid, indicate all the elements but titanium. These are probably the $CaO \cdot MgO \cdot SiO_2$ primary phase. According to Berezhnoi's[40e] composition tetrahedron, the $CaO \cdot MgO \cdot SiO_2$ primary field will be next to the MgO primary field, and the $CaO \cdot MgO \cdot SiO_2$ phase will precipitate out during cooling as the liquid moves along the MgO-$CaO \cdot MgO \cdot SiO_2$ boundary line. The rest of the liquid, where a fine eutectic structure is observed, is the portion of the drop which freezes at the invariant point.

The photomicrograph of the sample of 30% TiO_2 containing liquid is shown in Fig. 15. Again, from a comparison of this micrograph with the oscilloscope traces of the elements given in Fig. 11(b), the white regions are identified as the $CaO \cdot TiO_2$ phase. The dark gray regions appear to be the $2MgO \cdot SiO_2$ phase since they contain no calcium and titanium. The rest could not be identified clearly. In both of these samples some titanium in the substrate could be detected, although as in the Al_2O_3-MgO-$CaO \cdot SiO_2$ system, most of this would be due to the background effect.

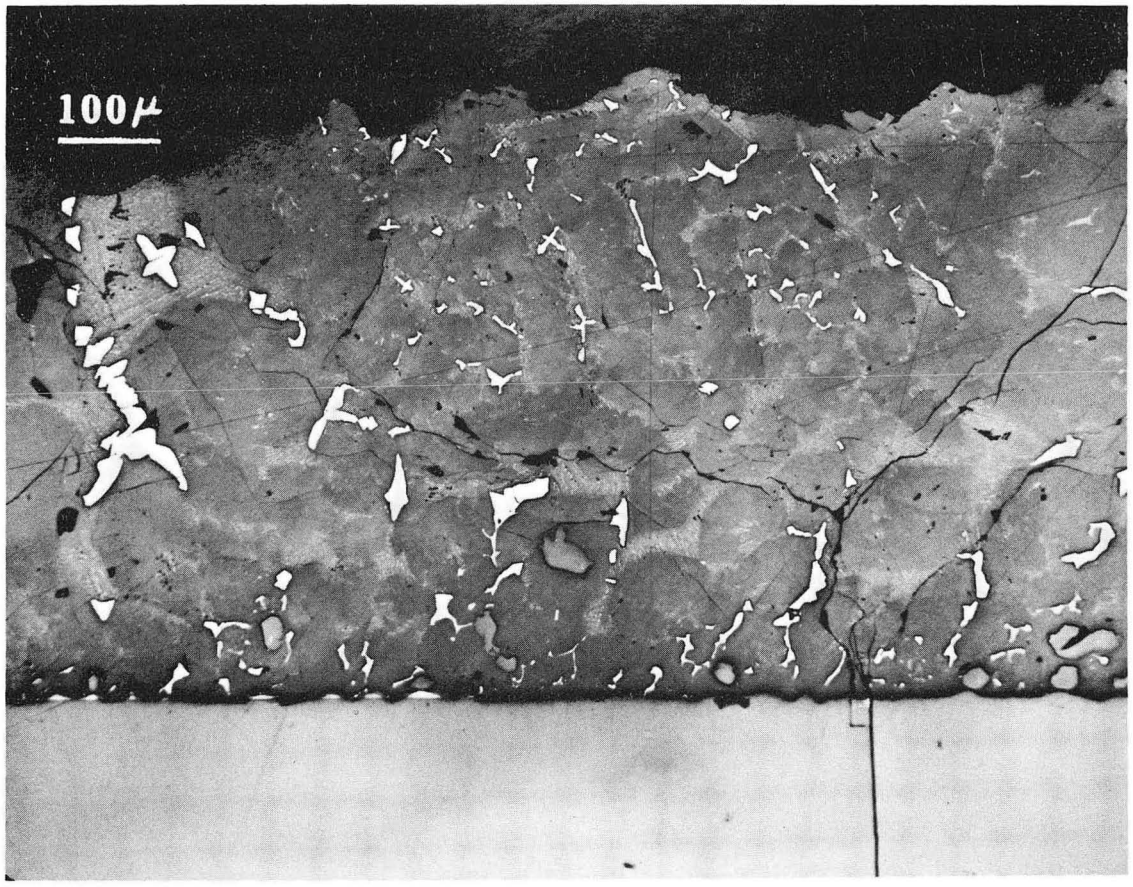

XBB 6810-6118

Fig. 14 Solid liquid interface of the sample with an original drop composition of 5% TiO_2 + 95% CMS, held 3 hours at 1550°C.

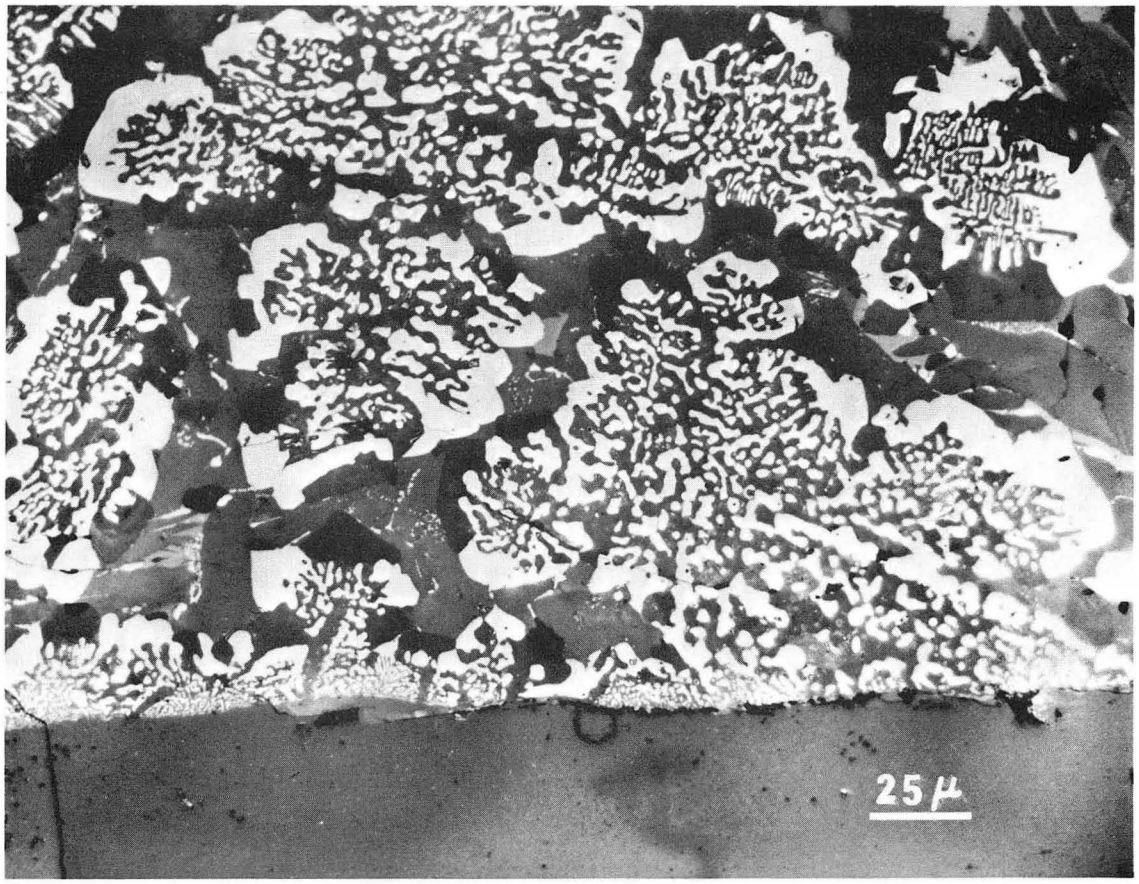

XBB 6810-6117

Fig. 15 Solid liquid interface of the sample with an original drop composition of 30% TiO_2 + 70% CMS, held 3 hours at 1550°C.

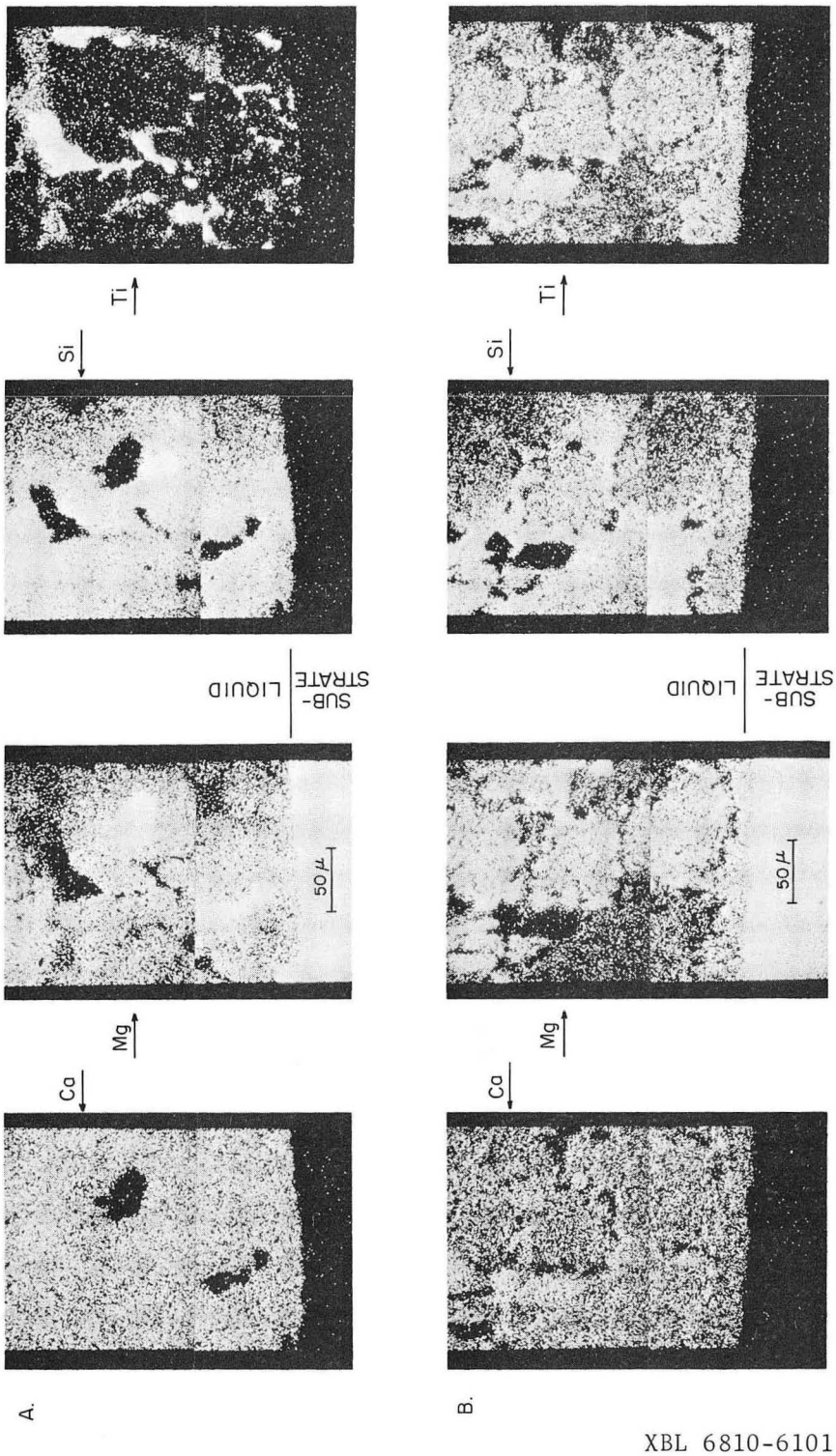

XBL 6810-6101

Fig. 16 Oscilloscope traces of the solid liquid interfaces of the samples with original drop compositions of (a) 5% TiO_2 + 95% CMS, and (b) 30% TiO_2 + 70% CMS, held 3 hours at 1550°C.

D. Nature of Interface Reactions and Their Effect on Contact Angle

The interface reactions discussed in the preceding sections can be classified under three general groups:

(a) The liquid dissolves MgO from the substrate surface when it is unsaturated with respect to MgO,

(b) If the liquid is saturated with respect to $MgO \cdot R_2O_3$, but not with MgO, the MgO of the substrate reacts with the R_2O_3 of the liquid to form spinel, and

(c) The MgO of the substrate reacts with R_2O_3 or TiO_2 of the liquid to form a solid solution.

A hypothetical R_2O_3-MgO-$CaO \cdot SiO_2$ ternary phase diagram, shown in Fig. 17, will be used to discuss the nature of these interface reactions. Although the iron oxide-MgO-$CaO \cdot SiO_2$ system is a quaternary system, the use of this simplified diagram will not alter the discussion on the interface reactions. Furthermore, in this R_2O_3-MgO-$CaO \cdot SiO_2$ system, the discussion of the behavior of a drop composition "L_T" on the MgO substrate will be sufficient to cover all the different cases encountered in this study.

At a temperature "T_1," the premelted drop of the composition "L_T" contains solid particles of $MgO \cdot R_2O_3$ and a liquid of composition "L." When this drop is on a pure MgO substrate, the liquid composition will shift from L to L' by dissolving MgO from the substrate surface. The liquid composition will next tend to move into the MgO primary field along the T_1 isotherm as it loses some of its R_2O_3 to the substrate since all of the R_2O_3's formed solid solution with MgO. However, if the spinel particles of the drop can make up for this loss by dissolving in the

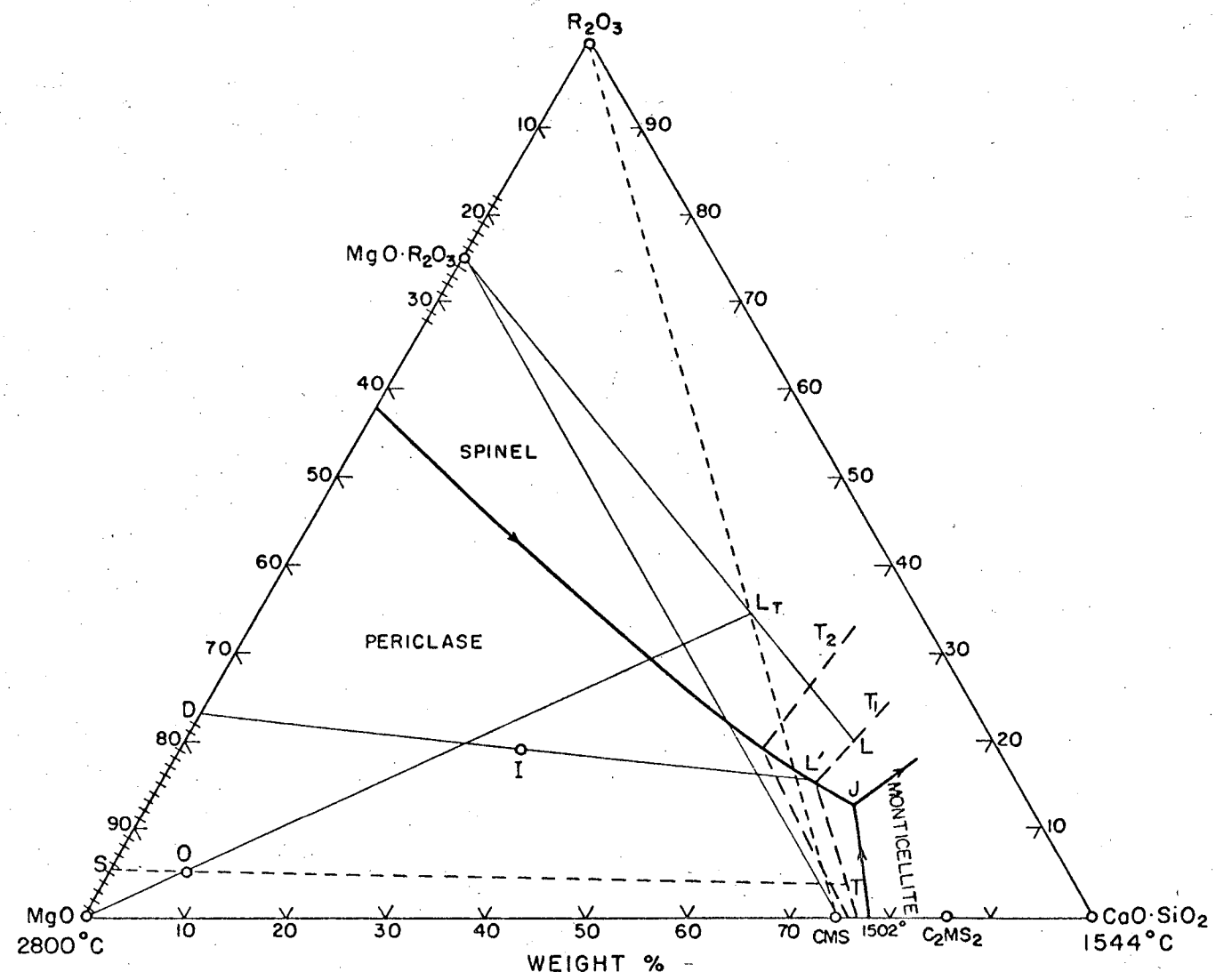

XBL 6810-6030

Fig. 17. Hypothetical R_2O_3-MgO-CaO.SiO_2 equilibrium phase diagram.

liquid faster than the substrate can react with the R_2O_3 of the liquid, the composition should stay at L' until all of the spinel in the drop is depleted. The liquid composition will then shift into the MgO primary field only after the excess spinel of the drop is depleted.

The overall composition of the drop-substrate system can be represented by a point "O" on the line joining L_T to MgO. This point will be closer to the MgO side since the mass of the substrates used was considerably larger than that of the drops. As the overall drop composition changes from L_T to L' and subsequently moves into the MgO primary field, the overall substrate composition moves towards a saturated solid solution composition represented by point D for temperature T_1. During this adjustment period, the liquid and the substrate compositions will be joined by the dash line which rotates with point O as a fulcrum. This adjustment will cease when the activity of R_2O_3 in the substrate becomes equal to that of the R_2O_3 in the liquid. At equilibrium, the substrate and the liquid will then be represented by equal R_2O_3 activity compositions S and T, respectively. In this study the equilibrium for the whole system was never attained since the time allowed for the diffusion of R^{3+} or R^{2+} cations into the MgO substrate was not long enough to attain the equilibrium structure. In the experiment with 56% Fe_2O_3 + 44% CMS liquid composition, for instance, the diffusion layer constituted only 20% of the substrate.

Although the system as a whole needs a long time to attain an equilibrium composition, the interface region itself can reach a transient equilibrium state rapidly. In the L_T-MgO system, for instance, if the interface reaction is not the rate controlling step, the substrate at the

interface will correspond to the saturation composition of D while the liquid is at L'. Then the interface region can be thought of as an isolated system containing equal amounts of liquid and substrate phases. The overall composition of this interface region will be represented by point I.

The liquid L' can coexist in equilibrium with the MgO solid solution phase of composition D and with the spinel phase. If the liquid is in the spinel primary field, however, it reacts with the MgO solid solution to form more spinel. If the MgO solid solution is unsaturated, this liquid now reacts with the unsaturated MgO solid solution to form either spinel or saturated MgO solid solution, as given by the following reactions:

$$R_2O_3(\text{in liquid}) + MgO\text{-}R_2O_3(\text{subst., unsat.ss}) \rightarrow MgO\text{-}R_2O_3(\text{sat.ss}) \quad (3)$$

$$R_2O_3(\text{in liquid}) + MgO\text{-}R_2O_3(\text{subst., unsat.ss}) \rightarrow MgR_2O_4(\text{spinel}) \quad (4)$$

The magnitude of $(-)\Delta G$, in both cases, is directly proportional to the degree of undersaturation of the $MgO\text{-}R_2O_3$ solid solution. Thus, one would expect ΔG_3 and ΔG_4 to be the same. In sessile drop experiments, when the substrate at the interface is an unsaturated solid solution and the liquid is in the spinel primary field, both of these reactions can take place. The growth rate of the products, however, will determine which one of these two phases will grow at the interface.

Once the liquid reaches L' and begins to move into the MgO primary field, the liquid and the substrate can react to form only the saturated MgO solid solution phase as given by reaction (3). The $(-)\Delta G$ of the reaction now decreases as the liquid composition changes to a lower R_2O_3 content.

Under equilibrium conditions, the contact angle in Young's equation is determined by a balance of interfacial and surface tensions acting on the periphery of the drop. Under non-equilibrium conditions, however, the use of this equation becomes inappropriate since the interfacial and surface tensions will be changing continuously as the whole system adjusts itself towards a lower free energy configuration. The nature of the interface reactions now plays a very important role in the behavior of the liquid.

If the liquid is in the spinel primary field, under unsteady state conditions the ΔG for reactions (3) and (4) will have a high negative value immediately after the first portion of the liquid forms on the substrate. This is due to the initial high undersaturation of the substrate. As the reaction proceeds, the degree of undersaturation of the substrate, and consequently, the driving force of the reaction will decrease. Around the periphery of the drop, however, where the liquid is next to an undersaturated $MgO-R_2O_3$ solid solution, the liquid will advance further to react with more MgO. When the driving force for this reaction is high, the liquid can wet the substrate completely before the steady state conditions are attained. If the kinetics are such that the substrate surface around the periphery of the drop can approach the saturation composition rapidly, the driving force for the reaction becomes low. The liquid then stops at a finite steady state angle when the liquid surface cannot be stretched any further.

The steps which might play an important role in the kinetics of this wetting phenomenon are:

(a) Dissolution of spinel in the liquid,

(b) Diffusion of R^{3+} or R^{2+} cations in the liquid,

(c) Interface reaction,

(d) Diffusion of R^{3+} or R^{2+} cations in the substrate, and

(e) Dissolution of MgO in the liquid.

The diffusion of R^{3+} or R^{2+} cations in the liquid will not be expected to be a rate controlling step because the diffusion in the liquid will be much faster than that in the substrate. If (a) is the rate controlling step, the R_2O_3 content of the liquid around the periphery will be depleted as diffusion into the substrate continues. Once the liquid reaches L' and subsequently becomes undersaturated with respect to MgR_2O_4, reaction (3) will be the only possible interface reaction. The magnitude of $(-)\Delta G$ for this reaction will now decrease as the liquid approaches a pure CMS composition. If the interface reaction is the rate controlling step, the substrate will always be undersaturated while the liquid stays saturated. The magnitude of $(-)\Delta G$ will then be high. The magnitude of $(-)\Delta G$ will become low again if the diffusion of R^{3+} or R^{2+} cations in the substrate is the rate controlling step since now, the interface region of the substrate also becomes saturated. Finally, if the dissolution rate of MgO in the liquid is low, the above argument still applies unless the dissolution rate of spinel in the liquid is also slow. Then, as the liquid becomes depleted of R_2O_3, it will move along an almost constant MgO direction instead of following the T_1 isotherm.

In the Al_2O_3-MgO-CaO·SiO_2 and Fe_2O_3-FeO-MgO-CaO·SiO_2 systems in excess of 3% R_2O_3, the steady state contact angles would be 35° and 15°, respectively. On the other hand in the Cr_2O_3-MgO-CaO·SiO_2 and

TiO_2-MgO-$CaO \cdot SiO_2$ systems, the steady state contact angles become very low as the amount of Cr_2O_3 and TiO_2 are increased. These angles are indicated as zero in Fig. 2 since, in each case, the substrate was wetted completely. Attempts were later made to determine this very low contact angle with Cr_2O_3 additions at 1550°C. The biggest MgO substrates available were used while the size of the drops was decreased considerably. After 3 hours a contact angle of 7° was obtained for the system with 3% Cr_2O_3 + 97% CMS liquid composition. With the 5% Cr_2O_3 + 95% CMS liquid, the angle was 6° after 6 hours of heating. The contact angle could not be measured when the 15% Cr_2O_3 + 85% CMS liquid was fired on MgO for 3 hours since the drop segregated into very small segments around the trace of the original drop. Apparently, as the Cr_2O_3 content of the drop was depleted, the liquid tried to pull back, and during this process it formed small segments. With the 3% and 5% Cr_2O_3 containing liquids, the drops must also have spread first and pulled back as the Cr_2O_3 content in the drop decreased. In both cases the original drop traces were visible. For practical purposes, then, the liquids containing in excess of 3% Cr_2O_3 can be considered to spread on MgO. Yet this spreading was not obtained in the system with 4% $MgCr_2O_4$ + 96% CMS drop composition (Table I).

At this stage, one more step must be added to the five rate controlling steps listed above, namely the solution of R_2O_3 from the MgO-R_2O_3 solid solution in the liquid. This step plays an important part if the amount of MgO-R_2O_3 solid solution particles in the liquid is high and the solution rate of R_2O_3 at the (MgO-R_2O_3)-liquid interface is slow. In the 4% $MgCr_2O_4$ + 96% CMS liquid, the percentage of MgO-Cr_2O_3 solid

solution particles at test temperature is slightly higher than that in the 3% Cr_2O_3 + 97% CMS liquid. Although the former system, as a whole, contains more than 3% Cr_2O_3, the percentage of Cr_2O_3 in the liquid portion is actually less than that of the latter system. This percentage will decrease further after the liquid forms if the solution rate of Cr_2O_3 at the (MgO-Cr_2O_3)-liquid interface is slow. Thus, a finite steady state contact angle corresponding to a liquid composition less than 3% Cr_2O_3 is obtained instead of spreading.

In the literature, unfortunately, only limited data are available on the kinetics of the possible rate controlling steps outlined above. The diffusion rate of Fe^{2+} cations in MgO has been determined by Tagai, et al.[50] and Blank.[38] Tagai, et al., and recently Greskovich and Stubican[51] have determined the diffusion rate of Cr^{3+} cations in MgO. No data could be found on the kinetics of aluminum cation diffusion in MgO. Furthermore, the kinetics of the other steps still remain to be investigated.

According to Tagai, et al., at 1600°C Fe^{2+} and Cr^{3+} cation diffusivities in MgO are 3.1×10^{-9} and 1.3×10^{-11} $cm^2/sec.$, respectively. If the diffusion of cations in MgO is the rate controlling step within the first second of the diffusion, the activity profiles of Fe_2O_3 and Cr_2O_3 in MgO will be as shown in Fig. 18. In order to plot these activity profiles, the concentration profiles of Fe_2O_3 and Cr_2O_3 in MgO were first determined using Tagai, et al.'s diffusivity data. Assuming that the MgO-Fe_2O_3 and MgO-Cr_2O_3 solid solutions are ideal, the activities can be obtained directly from the concentration profiles. A comparison of these profiles shows that for a given time the interface region of the substrate around the periphery in the Fe_2O_3 containing systems would

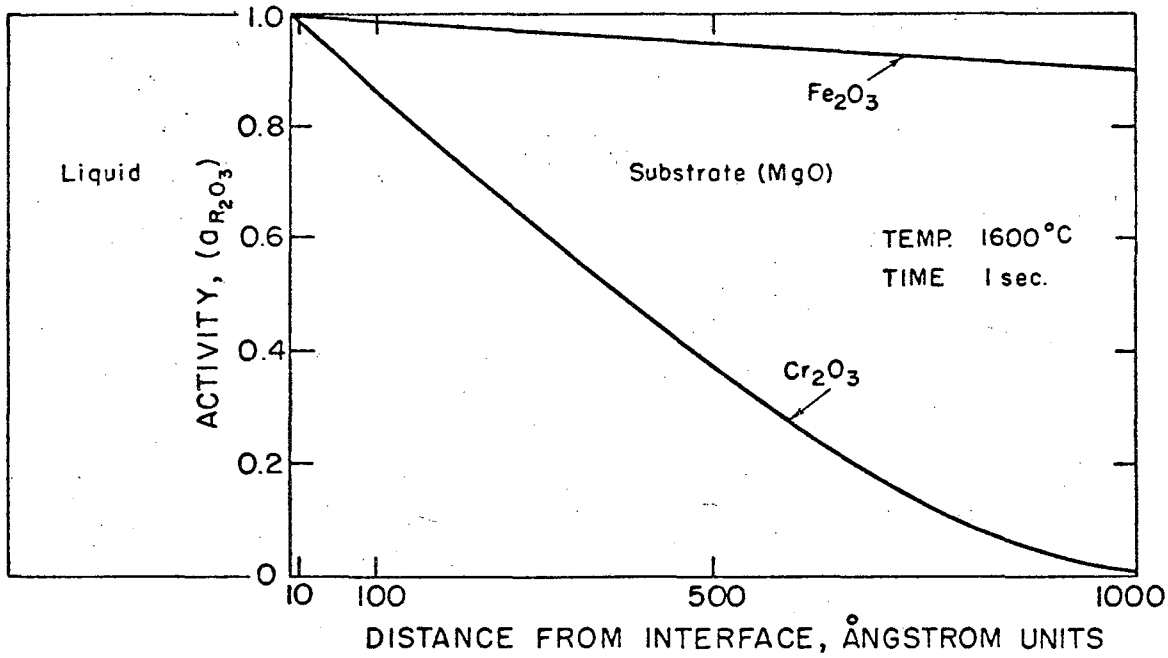

XBL 6810-6027

Fig. 18. Activity profiles of Fe_2O_3 and Cr_2O_3 in MgO solid solution, after 1 sec at 1600°C.

reach saturation much faster than it would in the Cr_2O_3 containing systems. If an effective interface region of 100 Å can be assumed, ΔG_3 and ΔG_4 at the interface will have a higher negative value in the Cr_2O_3 containing systems than it will in the Fe_2O_3 containing systems. Under these conditions, then, one would expect the Cr_2O_3 containing liquids to spread more on a MgO substrate.

The kinetics of aluminum cation diffusion in MgO is yet to be determined. A fast aluminum cation diffusion in MgO could be a contributing factor to the relatively high steady state contact angle observed. The microscope studies, however, indicated that the dissolution rate of $MgAl_2O_4$ spinel in the liquid could also be an important factor to consider. In Fig. 19, the periphery region of a drop with an original composition of 30% Al_2O_3 + 70% CMS is shown. The angular particles are $MgAl_2O_4$ spinel. It appears that the periphery region of the liquid is almost completely depleted of excess spinel after 3 hours at 1550°C. This phenomenon which was not observed in the other systems would be due to a slow dissolution rate of $MgAl_2O_4$ spinel in the liquid. Thus, at steady state the contact angle corresponds to a finite value since the $(-)\Delta G$ of the interface reaction around the periphery region will be low. Similarly, in the TiO_2-MgO-$CaO \cdot SiO_2$ system the formation of a solid solution at the interface would be a contributing factor to the lowering of the contact angle. In this case, since the liquids dissolve MgO from the surface, the driving force for this reaction may also contribute to the decrease in the contact angle. Apparently with 5% TiO_2 containing liquid, this dissolution step was short since the presence of MgO particles in the drop indicates that the liquid was already at equilibrium

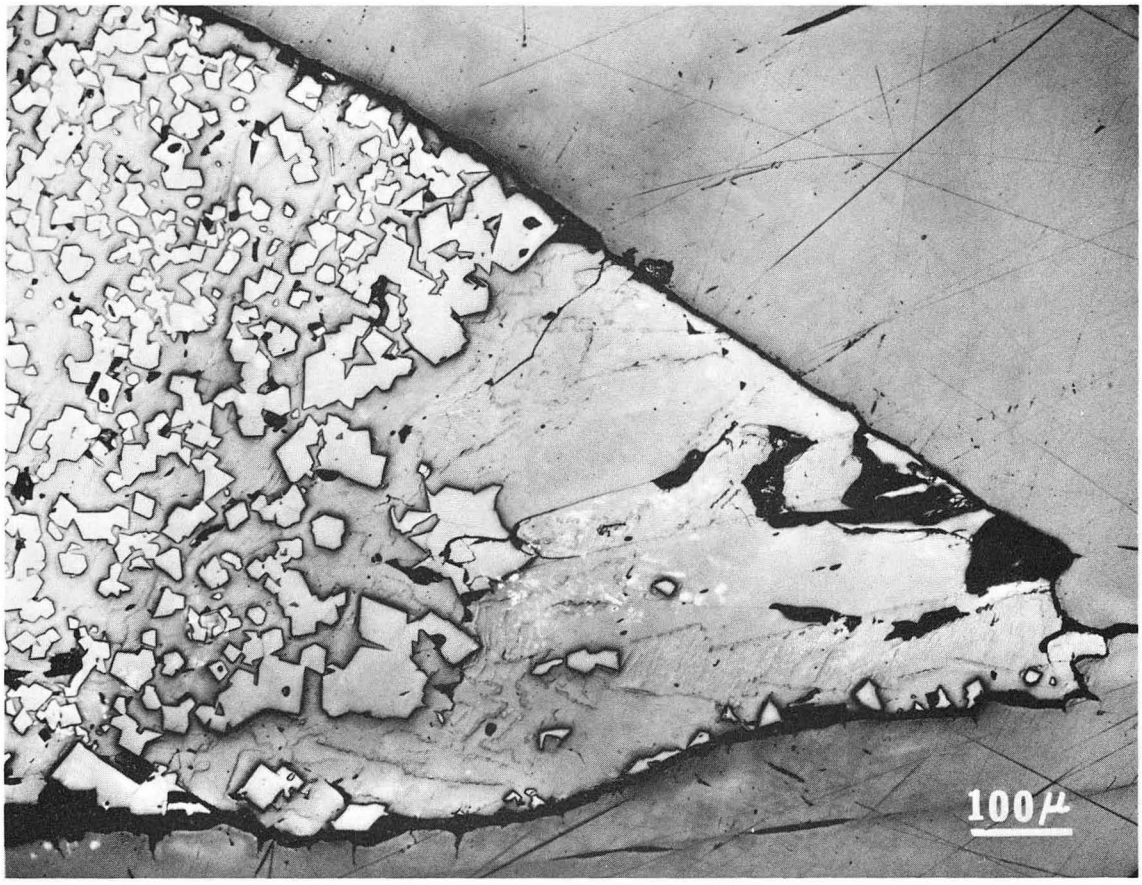

XBB 6810-6119

Fig. 19 Periphery region of the sessile drop with an original composition of 30% Al_2O_3 + 70% CMS, held 3 hours at 1550°C.

with MgO after 3 hours.

The macroscopic nature of the experiments in this study was the primary cause for the delay in reaching the final equilibrium states. In a compact, however, where the solid particles are usually micron size, the equilibrium configuration will be readily achieved. The dihedral angle measurements of Jackson, et al.,[4] and Jackson and Ford[5] in the periclase-monticellite system corresponded to this equilibrium configuration. In their studies, a firing period of one hour was adequate to reach equilibrium. Finite dihedral angles were obtained between the MgO grains. If shorter firing periods corresponding to the non-equilibrium stage were used, either the dihedral angles would have been very low or the MgO grains would have been completely surrounded by the liquid. This transient wetting stage would be due to the reactions at the solid-liquid interface.

V. CONCLUSIONS

The contact angle of monticellite ($CaO \cdot MgO \cdot SiO_2$) liquid on (100) faces of magnesium oxide at 1550°C was determined to be in the range of 43-51°. The Al_2O_3, Cr_2O_3, Fe_2O_3, and TiO_2 additions to the liquid, in each case, resulted in a decrease in the contact angle. Spreading was obtained with Cr_2O_3 and TiO_2 additions (Fig. 2).

The equilibrium structure of the monticellite-magnesium oxide system is disturbed with additions of Al_2O_3, Cr_2O_3, Fe_2O_3, and TiO_2. The system then goes through a transient non-equilibrium stage. During this stage, a driving force exists for reactions at the liquid-substrate interface to achieve an equilibrium structure. The degree of wetting is directly proportional to the degree of this driving force, or the magnitude of $(-)\Delta G$ for the reaction. Spreading is obtained when the magnitude of $(-)\Delta G$ for the reaction is high resulting in a wetting driving force that exceeds the surface tension of the liquid.

The wetting phenomenon in this transient stage is affected by the kinetics of: (a) dissolution of spinel in the liquid, (b) diffusion of additive cations in the liquid, (c) interface reaction, (d) diffusion of additive cations in the substrate, and (e) dissolution of MgO in the liquid.

The goal of this study which was to determine the effect of Cr_2O_3, Fe_2O_3, Al_2O_3, and TiO_2 on the solid-liquid interfacial energy of the equilibrium periclase-monticellite system was not achieved. The final equilibrium compositions could not be attained due to the macroscopic nature of the experiments. Therefore, the reported contact angles are not the equilibrium contact angles but the steady state angles of a

transient reaction stage. In order to measure the equilibrium contact angles, one then has to perform the sessile drop experiments on substrates that are initially at equilibrium with the liquid.

Nevertheless, the results of this study are quite valuable since they provide a greater understanding of the role of interface reaction kinetics in sessile drop experiments. It is felt that the kinetics of interface reactions would play an equally important role in the microstructure development of a compact.

ACKNOWLEDGEMENTS

The author wishes to express his sincere appreciation for the patient guidance of Professor Joseph A. Pask.

The counsel of Professor Leo Brewer was very helpful during the course of this research project.

It is with sincere thanks that the author acknowledges the contributions of his fellow students in the completion of this work, particularly, Messrs. Robert F. Davis and John J. Brennan. The technical aid of Messrs. George Dahl and George Georgakopoulous was invaluable, as was the secretarial assistance of Miss Kelly Radmilovic.

The author's research was supported by the United States Atomic Energy Commission.

APPENDIX

1. The Chemical Analysis of MgO Powder

Baker and Adamson Reagent No. 1917

Substance	Wt. %
Assay (MgO) (after ignition)	99.0
Insoluble in dilute HCl	0.020
Soluble in water	0.40
Loss on ignition	2.0
Ammonium hydroxide precipitate	0.020
Chloride (Cl)	0.010
Nitrite (NO_3)	0.005
Sulfate and sulfite (as SO_4)	0.005
Barium (Ba)	0.005
Calcium (Ca)	0.05
Heavy metals (as Pb)	0.003
Iron (Fe)	0.010
Manganese (Mn)	0.0005
Potassium (K)	0.005
Sodium (Na)	0.50
Stronium (Sr)	0.005
Silica (SiO_2)	0.040

2. The Chemical Analysis of $CaCO_3$ Powder

Baker and Adamson Reagent No. 1506

Substance	Wt. %
Assay ($CaCO_3$)	99.0
Insoluble in dilute HCl	0.010
NH_4OH precipitate	0.010
Chloride (Cl)	0.001
Oxidizing substance (as NO_3)	0.005
Sulfate (SO_4)	0.010
Ammonium (NH_4)	0.003
Barium (Ba)	0.005
Stronium (Sr)	0.10
Magnesium (Mg)	0.02
Potassium (K)	0.01
Sodium (Na)	0.10
Heavy metals (as Pb)	0.001
Iron (Fe)	0.002

3. SiO_2 Powder

Ottawa Silica Flour

Substance	Wt. %
Silica (SiO_2)	99.8
Alumina (Al_2O_3)	0.1
Iron oxide (Fe_2O_3)	0.02
Calcium oxide and magnesium oxide (CaO, MgO)	0.1

4. The Chemical Analysis of Al_2O_3 Powder

Baker Analyzed Reagent No. 0536

Substance	Wt. %
Assay (Al_2O_3)	99.5
Loss on ignition	0.3
Chloride (Cl)	0.005
Sulfate (SO_4)	0.003
Heavy metals (as Pb)	0.0005
Iron (Fe)	0.001

5. Cr_2O_3 Powder

Baker Analyzed Reagent No. 1616. A chemical analysis was not performed.

6. The Chemical Analysis of Fe_2O_3 Powder

Baker Analyzed Reagent No. 2024

Substance	Wt. %
Assay (Fe_2O_3)	99.5
Insoluble in HCl	0.04
Phosphate (PO_4)	0.02
Sulfate (SO_4)	0.04
Copper (Cu)	0.003
Manganese (Mn)	0.03
Substances not precipitated by NH_4OH (as SO_4)	0.003
Zinc (Zn)	0.003

7. The Chemical Analysis of TiO_2 Powder

Baker Analyzed Reagent No. 4162

Substance	Wt. %
Water soluble salts	0.01
Arsenic (As)	0.0001
Iron (Fe)	0.001
Lead (Pb)	0.008
Zinc (Zn)	0.005

8. The Spectroscopic Analysis* of MgO Single Crystals

Substance	Wt. % Oxide
Magnesium (Mg)	Principle Constituent
Iron (Fe)	0.015
Aluminum (Al)	0.007
Chromium (Cr)	0.002
Titanium (Ti)	Not detected
Silicon (Si)	<0.005
Calcium (Ca)	0.01
Manganese (Mn)	0.001
Nickel (Ni)	Not detected

* The analysis was performed by the American Spectrographic Laboratories, Inc., 557 Minna Street, San Francisco, California

REFERENCES

1. W. F. Ford, A. Hayhurst and J. White, "The effect of bond structure on the high temperature tensile behavior of basic bricks," Trans. Brit. Ceram. Soc., 60 [8] 581-601 (1961).

2. L. H. Van Vlack, "Microstructure of silica in the presence of iron oxide," J. Am. Ceram. Soc., 43 [3] 140-45 (1960).

3. C. S. Smith, "Grains, phases and interfaces: an interpretation of microstructure," Trans. AIME, 175 [1] 15-51 (1948).

4. B. Jackson, W. F. Ford, and J. White, "The influence of Cr_2O_3 and Fe_2O_3 on the wetting of periclase grains by liquid silicate," Trans. Brit. Ceram. Soc., 62 [7] 577-601 (1963).

5. B. Jackson and W. F. Ford, "A quantitative study of bonding in basic refractories," Trans. Brit. Ceram. Soc., 65 [1] 19-39 (1966).

6. W. D. Kingery and M. Humenik, Jr., "Surface tension at elevated temperatures. I. Furnace and method for use of the sessile drop method; surface tension of silicon, iron and nickel," J. Phys. Chem., 57 [3] 359-63 (1953).

7. P. Kozakévitch, "Surface tension of liquid metals and oxide melts," Liquids: Structure, Properties Solid Interactions, Thomas J. Hughel (Ed.), Elsevier Publishing Co., Amsterdam, 1965.

8. F. A. Halden and W. D. Kingery, "Surface tension at elevated temperatures. II. Effect of C, N, O and S on liquid iron surface tension and interfacial energy with Al_2O_3," J. Phys. Chem., 59 [6] 557-59 (1955).

9. C. R. Kurkjian and W. D. Kingery, "Surface tension at elevated temperatures. III. Effect of Cr, In, Sn and Ti on liquid nickel surface tension and interfacial energy with Al_2O_3," J. Phys. Chem., 60 [7] 961-63 (1956).

10. B. C. Allen and W. D. Kingery, "Surface tension and contact angles in some liquid metal-solid ceramic systems at elevated temperatures," Trans. AIME, 215 [1] 30-37 (1959).

11. W. D. Kingery, "Metal-ceramic interactions: I, Factors affecting fabrication and properties of cermet bodies," J. Am. Ceram. Soc., 36 [11] 362-65 (1953).

12. G. Economos and W. D. Kingery, "Metal-ceramic interactions: II, Metal-oxide interfacial reactions at elevated temperatures," J. Am. Ceram. Soc., 36 [12] 403-09 (1953).

13. M. Humenik, Jr. and W. D. Kingery, "Metal-ceramic interactions: III, Surface tension and wettability of metal-ceramic systems," J. Am. Ceram. Soc., 37 [1] 18-23 (1954).

14. W. D. Kingery, "Metal-ceramic interactions: IV, Absolute measurement of metal-ceramic interfacial energy and the interfacial adsorption of silicon from iron-silicon alloys," J. Am. Ceram. Soc., 37 [2] 42-45 (1954).

15. W. M. Armstrong, A. C. D. Chaklader, and J. F. Clarke, "Interface reactions between metals and ceramics: I, Sapphire-nickel alloys," J. Am. Ceram. Soc. 45 [3] 115-18 (1962).

16. W. M. Armstrong, A. C. D. Chaklader, and M. L. A. DeCleene, "Interface reactions between metals and ceramics; II, Refractory metals - fused SiO_2 system," J. Am. Ceram. Soc., 45 [9] 407-12 (1962).

17. W. M. Armstrong, A. C. D. Chaklader, and D. J. Rose, "Interface reactions between metals and ceramics, part III: MgO-Fe alloy system," Trans. AIME, 227 [5] 1109-15 (1963).

18. A. C. D. Chaklader, A. M. Armstrong, and S. K. Misra, "Interface reactions between metals and ceramics: IV, Wetting of sapphire by liquid copper-oxygen alloys," J. Am. Ceram. Soc., 51 [11] 630-33 (1968).

19. J. A. Pask and R. M. Fulrath, "Fundamentals of glass-to-metal bonding: VIII, Nature of wetting and adherence," J. Am. Ceram. Soc. 45 [12] 592-96 (1962).

20. J. A. Pask, "Glass-Metal 'interfaces' and bonding," Modern Aspects of the Vitreous State, J. D. Mackenzie, (Ed.) Butterworths, London, 1964.

21. J. A. Pask and M. P. Borom, "Physical chemistry of glass-metal interfaces," UCRL-11816 Rev., May 1965.

22. L. H. Van Vlack, "Geometry of microstructures," Microstructures of Ceramic Materials, NBS, Miscellaneous Publication 257, Wash. D.C., 1964.

23. J. White, "The nature of the factors determining the structure of polyphase ceramics," Science of Ceramics, G. H. Stewart, (Ed.) Vol. 2 pp 305-30, Academic Press, London and New York, 1965.

24. L. H. Van Vlack and O. K. Riegger, "Microstructures of magnesio-wüstite [(Mg,Fe)O] in the presence of SiO_2," Trans. AIME, 224 [5] 957-65 (1962).

25. O. K. Riegger, G. I. Madden, and L. H. Van Vlack, "The microstructures of periclase when subjected to steelmaking variables," Trans. AIME, 227 [5] 971-76 (1963).

26. L. H. Van Vlack and G. I. Madden, "Grain-growth restriction in two-phase microstructures," Trans. AIME, 230 [5] 1200-02 (1964).

27. D. S. Buist, B. Jackson, I. M. Stephenson, W. F. Ford and J. White, "The kinetics of grain growth in two-phase (solid-liquid) systems," Trans. Brit. Ceram. Soc., 64 [4] 173-209 (1965).

28. I. M. Stephenson and J. White, "Factors controlling microstructure and grain growth in two-phase (one solid + one liquid) and in three-phase (two solid + one liquid) systems," Trans. Brit. Ceram. Soc., 66 [9] 443-83 (1967).

29. B. H. Baker and P. Schroth, "High hot strength in basic brick," Bull. Am. Ceram. Soc., 47 [7] 623-26 (1968).

30. H. J. S. Kriek and B. B. Segal, "Effect of the silicate constitution of magnesite bricks on the high-temperature strength," Trans. Brit. Ceram. Soc., 66 [2] 65-83 (1967).

31. A. Hayhurst and J. Laming, "The structure of chrome-magnesite refractories at high temperatures," Trans. Brit. Ceram. Soc., 62 [12] 989-1005 (1963).

32. A. Hayhurst and J. Laming, "Modifications of microstructure of chrome-magnesite refractories by heat treatment," Trans. Brit. Ceram. Soc., 63 [3] 135-142 (1964).

33. Von K. Konopicky, "Structure of highly fired, so-called directly bonded, chromium ore-containing basic products," Ber. Dtsch. Keram. Ges., 44 [7] 333-37 (1967).

34. B. Brezny and Z. Smutny, "Mechanism of the formation of a direct bond between chrome spinel and periclase," Interceram, 16 [1] 32-35 (1967).

35. M. Humenik, Jr. and N. M. Parikh, "Cermets: I, Fundamental concepts related to microstructure and physical properties of cermet systems," J. Am. Ceram. Soc., 39 [2] 60-63 (1956).

36. N. M. Parikh and M. Humenik, Jr., "Cermets: II, Wettability and microstructure studies in liquid-phase sintering," J. Am. Ceram. Soc., 40 [9] 315-20 (1957).

37. A. P. Raju and J. A. Pask, "Observations on the development of microstructure in multiphase magnesia and forsterite bodies," Presented at the Basic Science Division Meeting of the Am. Ceram. Soc., September 20, 1968.

38. S. L. Blank, "The kinetics and mechanisms of the diffusion of iron and nickel in single crystals of magnesium oxide," (Ph.D. Thesis) UCRL-17411, March 1967.

39. J. J. Brennan, "The wetting of aluminum oxide by liquid aluminum," (M.S. Thesis) UCRL-17008, August 1966.

40. (a) E. F. Osborn and A. Muan, Figure 598 in Phase Diagrams for Ceramists, E. M. Levin, C. R. Robbins, and H. F. McMurdie, Am. Ceram. Soc., Ohio 1964.

(b) E. F. Osborn and A. Muan, Figure 630, ibid.

(c) W. F. Ford and W. J. Rees, Figure 924, ibid.

(d) A. S. Berezhnoi, Figure 927, ibid.

(e) A. S. Berezhnoi, Figures 930 and 934, ibid.

(f) F. Massazza and E. Sirchia, Figure 269, ibid.

(g) L. W. Coughanour and V. A. DeProsse, Figure 270, ibid.

41. A. M. Alper, "Microstructures developed from fusion casting," Ceramic Microstructures, R. M. Fulrath and J. A. Pask (Eds.), p. 767, John Wiley & Sons, Inc., New York, 1968.

42. D. M. Roy, R. Roy, and E. F. Osborn, "The system $MgO-Al_2O_3-H_2O$ and influence of carbonate and nitrate ions on the phase equilibria," Am. J. Sci., 251, 337-61 (1953).

43. A. M. Alper, R. N. McNally, P. H. Ribbe, and R. C. Doman, "The system $MgO-MgAl_2O_4$," J. Am. Ceram. Soc., 45 [6] 263-68 (1962).

44. R. M. El-Shahat and J. White, "Phase-equilibrium relationships in spinel-silicate systems, II, The pseudo-systems $MgAl_2O_4$ - $MgCr_2O_4$ - $CaMgSiO_4$, $MgFe_2O_4$ - $MgCr_2O_4$ - $CaMgSiO_4$, $MgAl_2O_4$ - $MgFe_2O_4$ - $CaMgSiO_4$, and $MgAl_2O_4$ - $MgFe_2O_4$ - $MgCr_2O_4$ - $CaMgSiO_4$," Trans. Brit. Ceram. Soc., 65 [6] 309-36 (1966).

45. E. F. Osborn, R. C. DeVries, K. H. Gee, and H. M. Kraner, "Optimum composition of blast furnace slag as deduced from liquidus data for the quaternary system CaO - MgO - Al_2O_3 - SiO_2," Trans. AIME, 200 33-45 (1954).

46. A. M. Alper, R. N. McNally, R. C. Doman, and F. G. Keihn, "Phase equilibria in the system MgO - $MgCr_2O_4$," J. Am. Ceram. Soc., 47[1] 30-33 (1964).

47. W. T. Wilde and W. J. Rees, "The ternary system MgO - Al_2O_3 - Cr_2O_3," Trans. Brit. Ceram. Soc., 42, 126-55 (1943).

48. F. P. Glasser and E. F. Osborn, "Phase equilibrium studies in the system CaO - Cr_2O_3 - SiO_2," J. Am. Ceram. Soc., 41 [9] 362 (1958).

49. J. C. Willshee and J. White, "Am investigation of equilibrium relationships in the system MgO - FeO - Fe_2O_3 up to 1750°C in air," Trans. Brit. Ceram. Soc., 66 [11] 541-55 (1967).

50. Von H. Tagai, S. Iwai, T. Iseki, and M. S. Tokio, "Diffusion of iron, manganese and chromium oxides into single crystal magnesia," Radex-Rundschau, 4, 577-83 (1965).

51. C. Greskovich and V. S. Stubican, "Interdiffusion studies in the system MgO - Cr_2O_3," J. Phys. & Chem. Solids, (to be published).

TECHNICAL INFORMATION DIVISION
LAWRENCE RADIATION LABORATORY
UNIVERSITY OF CALIFORNIA
BERKELEY, CALIFORNIA 94720